

# **A Role for the Orphan Serine hydrolase CG17192 in the *Drosophila* immune response**

A Master's Thesis

submitted to

Indian Institute of Science Education and Research Pune in partial fulfilment of the  
requirements for the BS-MS Dual Degree Programme

by

**Mrunal Ashok Pazare**



Indian Institute of Science Education and Research Pune

Dr. Homi Bhabha Road, Pashan, Pune 411008, INDIA.

Date: 10<sup>th</sup> April 2023

Under the guidance of  
Prof. Girish Ratnaparkhi,  
Professor, Department of Biology

From May 2022 to Mar 2023

© Mrunal Pazare  
All rights reserved

## Certificate

This is to certify that this dissertation entitled **A Role for the Orphan Serine hydrolase CG17192 in the *Drosophila* immune response** towards the partial fulfilment of the BS-MS dual degree programme at the Indian Institute of Science Education and Research, Pune represents work carried out by **Mrunal Ashok Pazare** at **Indian Institute of Science Education and Research** under the supervision of **Prof. Girish Ratnaparkhi, Professor, Department of Biology**, during the academic year **2022-2023**.



Prof. Girish Ratnaparkhi

Professor

Department of Biology

IISER Pune

Committee:

Guide : Prof. Girish Ratnaparkhi

TAC member: Dr. Amrita Hazra

This thesis is dedicated to all the individuals who have supported and encouraged me throughout my academic journey, without whom this project would not have been possible. That includes my family, friends, professors, and mentors who have provided me with guidance, inspiration, and unwavering support to help me reach this point.

## Declaration

I hereby declare that the matter embodied in the report entitled **A Role for the Orphan Serine hydrolase CG17192 in the *Drosophila* immune response** are the results of the work carried out by me at the **Department of Biology, Indian Institute of Science Education and Research, Pune**, under the supervision of **Prof. Girish Ratnaparkhi** and the same has not been submitted elsewhere for any other degree.



Mrunal Ashok Pazare  
20181184

Date:

## Table of Contents

<b>Declaration</b> .....	<b>4</b>
<b>Abstract</b> .....	<b>9</b>
<b>Acknowledgments</b> .....	<b>10</b>
<b>Chapter 1 Introduction</b> .....	<b>11</b>
Biochemical function of Serine Hydrolases.....	11
Catalytic Mechanism of Serine Hydrolases.....	12
Classification of Serine Hydrolase in <i>Drosophila melanogaster</i> .....	13
Role of Metabolic Serine Hydrolases.....	15
Lipases of Serine Hydrolases.....	16
CG17192: Biodata.....	17
Regulation of Dietary Lipid Uptake via CG17192: An Insight into the Molecular Mechanisms .....	19
Serine Hydrolyses: Key Players in Immune Defense Mechanisms .....	20
Innate Immunity in <i>Drosophila</i> .....	21
Serine Hydrolase in <i>Drosophila</i> Immunity .....	22
CG17192 in <i>Drosophila's</i> immunity .....	23
<b>Chapter 2 Materials and Methods</b> .....	<b>24</b>
SLiCE (seamless ligation cloning extract) based Cloning strategy .....	24
Oligos Designed for Cloning.....	25
Cloning of the gene CG17192 in the insect expression vector pRM .....	27
Transfection in Insect derived cells .....	28
Transformation and Protein Expression .....	29
Protein estimation using BCA (Bicinchoninic Acid).....	30
Gel-based ABPP: A Powerful Technique for qualitative analysis of serine hydrolases.....	30
Protein Purification under native condition.....	32
Bacterial Clearance Test.....	33
<b>Chapter 3 Results and Discussion</b> .....	<b>35</b>
PCR screening of recombinant plasmids .....	35
Sequencing confirms the insertion of the inserts in the plasmids.....	36
Protein expression of CG17192.....	40
Detection of CG17192 in the Soluble fraction.....	42
Optimizing protein expression of CG17192 in pET45b+ .....	43
Protein purification of CG17192 using Ni-NTA agarose beads.....	46
CG17192 is predicted to be secreted in the extracellular space .....	48

Validation of CG17192 Serine Hydrolase Activity .....	51
CG17192 shows immune suppression in the Midgut of the <i>Drosophila</i> .....	53
<b>References .....</b>	<b>57</b>

## List of Tables

<b>Table 1.</b> Gene Report describing Characteristic features of CG17192 obtained from FLYBASE .....	18
<b>Table 2.</b> Summary of CG17192 Gene Downregulation in Response to Various Infections...	23
<b>Table 3.</b> Primer sequences designed for insertion and site-directed mutagenesis of CG17192 in the bacterial expression vector, pET45b+ .....	26
<b>Table 4</b> Primer sequences designed for insertion and site-directed mutagenesis of CG17192 in the insect expression vector, pRM. ....	27
<b>Table 5.</b> PCR reaction volumes.....	28
<b>Table 6.</b> PCR temperature profile .....	28
<b>Table 7.</b> Fly lines with genetic mutations .....	33
<b>Table 8.</b> Successfully cloned Constructs .....	39

## List of Figures

<b>Figure 1.</b> Catalytic mechanism of a Serine Hydrolase (SH) reaction.....	13
<b>Figure 2.</b> Subfamilies of Serine Hydrolases.....	15
<b>Figure 3.</b> Diverse roles of Lipases.....	17
<b>Figure 4.</b> Regulatory mechanism of E78A in controlling the uptake of dietary lipids through CG17192.....	20
<b>Figure 5.</b> Haemocyte-mediated immunity in insects.....	22
<b>Figure 6.</b> Schematic of clone designed by SLiCE(seamless ligation cloning extract) based approach.....	24
<b>Figure 7.</b> Site Directed mutagenesis using SLiCE based approach for cloning.....	25
<b>Figure 8.</b> ABPP probes targeting the SH enzyme family.....	31
<b>Figure 9.</b> Schematic of the Activity based protein profiling (ABPP) workflow for bacterial lysates.....	31
<b>Figure 10.</b> Workflow of Bacterial Clearance Test (in case of <i>S. saprophyticus</i> ).....	34
<b>Figure 11.</b> PCR screening of recombinant Plasmids.....	35
<b>Figure 12.</b> Sequencing results of the insert in pET45b+.....	37
<b>Figure 13.</b> Sequencing results of the insert in pRM.....	38
<b>Figure 14.</b> Sequencing results of the insert in pRM with a FLAG tag.....	39
<b>Figure 15.</b> Western Blot analysis showing protein expression of the wildtype (CG17192) in the bacterial cells.....	41
<b>Figure 16.</b> Western Blot analysis showing protein expression of the mutant (CG17192 <sup>S179A</sup> ) in the bacterial cells.....	41
<b>Figure 17.</b> Immunoblot analysis successfully detects wildtype and mutant in the soluble protein fraction.....	42
<b>Figure 18.</b> Western Blot analysis showing protein expression of the CG17192 & mutant (CG17192 <sup>S179A</sup> ) in the bacterial cells.....	44
<b>Figure 19.</b> Western Blot analysis showing protein expression of the CG17192 in the bacterial cells.....	45
<b>Figure 20.</b> Coomassie-stained image showing protein expression of CG17192 in the bacterial cells.....	46
<b>Figure 21.</b> Purification under Native Conditions.....	47
<b>Figure 22.</b> Immunoblot and ponceau stained blots of protein purification steps.....	48
<b>Figure 23.</b> Signal sequence of CG17192.....	49
<b>Figure 24.</b> CG17192 protein expression in transfected S2 cells.....	50
<b>Figure 25.</b> The SDS-PAGE gel electrophoresis of pRM-CG17192-1x FLAG protein and pRM-CG17192 S179A-1x FLAG.....	50
<b>Figure 26.</b> ABPP Gel image of CG17192 & CG17192 S179A in the bacterial expression vector.....	51
<b>Figure 27.</b> ABPP Gel image of CG17192 & CG17192 <sup>S179A</sup> in the insect expression vector.....	52
<b>Figure 28.</b> ABPP Gel image of CG17192 & CG17192 <sup>S179A</sup> in the insect expression vector.....	53
<b>Figure 29.</b> Serine Hydrolases Do Not Contribute to the Resistance of <i>Staphylococcus saprophyticus</i> .....	54
<b>Figure 30.</b> CG17192 acts as a negative regulator of the host immunity.....	55



## Abstract

Highly conserved during evolution, the Serine Hydrolase (SH) superfamily of enzymes is a diverse group of catalysts that conduct a wide range of metabolic events in eukaryotic cells. A recent characterization of the activation of SHs in *Drosophila* (Kumar et al. 2021) found that the enzymatic activity of CG17192 is enriched in the female hemolymph and male gut. CG17192 is anticipated to be involved in degrading and absorbing a significant fraction (~ 30%) of adult triglycerides in the animal diet.

As part of my MS thesis project, I have initiated the functional characterization of CG17192 using in vitro biochemical assays, activity-based proteomics, and lipidomics. I have validated the activity of the SH in-vitro using ABPP (Activity-based protein profiling) assay, utilizing the broad-spectrum chemical probe fluorphosphonate tagged with either rhodamine. For in-vitro experiments, I have cloned CG17192 for expression in both bacteria and insect cells. Additionally, I have generated a catalytically dead CG17192<sup>S179A</sup> mutant. Loss of function studies in the midgut via RNAi indicate that CG17192 may function as an immunosuppressor.

## Acknowledgments

I extend my utmost appreciation to Prof. Girish Ratnaparkhi for his invaluable guidance and unwavering support throughout the course of the project. His mentorship has fostered my interest in research, and I am grateful for the freedom to explore and learn under his tutelage. Additionally, I am indebted to my thesis advisor, Dr. Amrita Hazra, for her insightful feedback and recommendations.

Furthermore, I am grateful to Kundan Kumar for sharing his lab expertise and mentorship and to Kamat Lab people for their provision of chemical compounds. Subhradip's instruction in my project has also been greatly appreciated. My heartfelt thanks go to the Fly facility at IISER Pune, without which this project would not have been possible.

I also extend my sincere appreciation to my lab colleagues Kundan, Rohith, Subhradip, Namrata, Lovleen, Sanhita, Amrita, Alex, Shruti, Prajna, Vidyadheesh, Raghunandan and Mukul for their constant support and the enjoyable atmosphere they have created.

In addition, I am deeply grateful to my friends, including Suyog, Avadhoot, Bhavesh, Aishwarya, Saket, Shruti, Kalyan, Sandesh, and Pushkar, for their unwavering love, care, support, and encouragement, without which a significant part of my experience at IISER would not have been possible.

Finally, I express my heartfelt thanks to my family, including my parents and sister, for their love, trust, and support. I would also like to acknowledge the Biology department of IISER Pune for providing me with the necessary facilities and opportunities and the DST-KVPY program for its financial support.

# Chapter 1 Introduction

Serine Hydrolases (SHs) are a class of enzymes that play a crucial role in a wide range of biological processes. This group of enzymes varies greatly but has a shared method of catalysis that involves the use of a serine residue as a nucleophile. This mechanism allows them to break down a broad range of substances, such as proteins, nucleic acids, carbohydrates, and lipids. (Bachovchin *et al.*, 2010). They are found in all domains of life (prokaryotic and eukaryotic) and play crucial roles in a variety of biological processes, including lipid metabolism (Braga *et al.*, 2006), digestion (Whitcomb and Lowe, 2007), and signalling pathways (Lane *et al.*, 2006).

## Biochemical function of Serine Hydrolases

The biochemical functions of serine hydrolases can vary depending on the specific enzyme and its location within the body, but some of the general functions they perform include the following:

**Lipid metabolism:** Many serine hydrolases are involved in the metabolism of lipids, including the breakdown of fats and the synthesis of phospholipids. For example, pancreatic lipase is a serine hydrolase that breaks down triglycerides in the intestine, while phospholipase A2 is involved in the breakdown of phospholipids in cell membranes (Shin *et al.*, 2019).

**Neurotransmitter regulation:** The nervous system's regulation of neurotransmitters also involves serine hydrolases. For example, acetylcholinesterase is a serine hydrolase that breaks down acetylcholine (the neurotransmitter), terminating its signal transmission.

**Regulation of endocannabinoids:** Endocannabinoids are molecules that occur naturally in the body and attach to cannabinoid receptors. Serine hydrolases play a role in regulating these molecules. One such example is fatty acid amide hydrolase (FAAH), which breaks down the endocannabinoid anandamide to regulate its levels in the body (Piomelli, 2003) (Savinainen *et al.*, 2012).

Overall, SHs play important roles in various biochemical processes and are essential for normal physiological functions.

## Catalytic Mechanism of Serine Hydrolases

Serine hydrolases are a class of enzymes that catalyzes the hydrolysis of amide, ester, and thioester bonds. They have a serine residue in their active site pocket that acts as a nucleophile in the catalytic mechanism (Long and Cravatt, 2011). Over 60% of SHs use an  $\alpha,\beta$ -hydrolase fold and implement a Ser-His-Asp catalytic triad (Holmquist, 2000). Nonetheless, there are various SH subclasses that utilize different folds and catalytic mechanisms, such as the amidase signature enzymes with a Ser-Ser-Lys triad (Shin *et al.*, 2002) (Bracey *et al.*, 2002) and patatin domain-containing lipases with a Ser-Asp dyad (Kienesberger *et al.*, 2009). These subclasses are evolutionarily distinct from one another.

The catalytic mechanism of SHs can be divided into three steps:

**The acyl-enzyme intermediate formation:** The enzyme's active site pocket holds onto the substrate, and the hydroxyl group (-OH) of the serine residue reacts with the substrate's carbonyl carbon, creating a tetrahedral intermediate. This produces an acyl-enzyme intermediate, where the substrate is attached to the serine residue through covalent bonding.

**Hydrolysis of the acyl-enzyme intermediate:** The active site pocket receives a water molecule which becomes activated through the influence of a histidine residue near the serine. Activated water molecule then initiates an attack on the acyl-enzyme intermediate's carbonyl carbon, causing the bond between the substrate and the serine residue to break. Consequently, the product is released as it undergoes hydrolysis, and the enzyme is regenerated, free to catalyze another reaction.

**Regeneration of the catalytic triad:** The histidine residue that activated the water molecule is now protonated by a nearby acidic residue, regenerating the active form of the histidine residue. Additionally, another serine residue in the active site donates a hydrogen atom to the oxygen of the serine residue that initially attacked the substrate, regenerating the active form of the serine residue. Overall, the catalytic mechanism of serine hydrolases involves the formation of an acyl-enzyme intermediate, the hydrolysis of this intermediate, and the regeneration of the active site residues necessary for catalysis (as represented in **Figure 1.**).

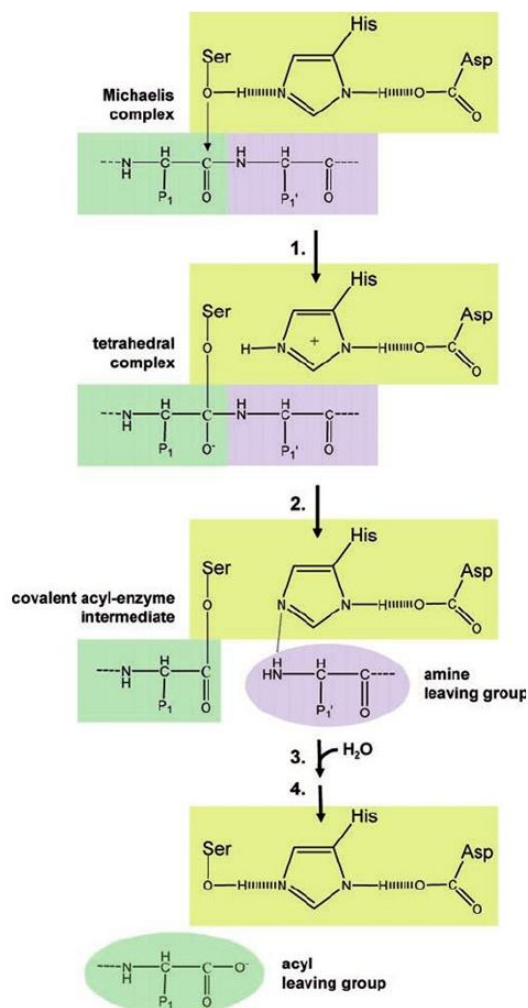


**Figure 1. Catalytic mechanism of a Serine Hydrolase (SH) reaction.**

The catalytic process of a SH reaction is illustrated in the above schematic. The catalytic triad, which plays a pivotal role in the reaction, is highlighted in yellow. Meanwhile, the substrate's amino- and carboxy-terminals adjacent to the scissile bond are depicted in green and purple colors correspondingly. Hydrogen bonds and polypeptide chain continuity of the substrate are indicated by broken lines. In step one of this two-step mechanism, an active-site serine attacks carbonyl Carbon at scissile bond while transferring its proton to histidine located within active site through facilitation by aspartate that stabilizes positive charge development during proton transfer. Subsequently, peptide bonding occurs via nitrogen atom when receiving donated proton (step two). In the initial stages of the reaction, the enzyme serine forms a covalent acyl intermediate with the amino-terminal portion of its substrate while simultaneously releasing its carboxy-terminal part. This process completes the acylation stage (steps 1 and 2). In contrast, during de-acylation (steps 3 and 4), water replaces the amine component of the substrate in an inverse sequence to that observed in acylation.

(Adapted from Schaller, 2005)

## Classification of Serine Hydrolase in *Drosophila melanogaster*

Serine hydrolases are a type of enzyme that cleave peptides and peptide bonds in proteins using a serine residue at their active site. This Family is classified into several sub-families based on their structure, substrate specificity, and mechanism of action. Some of the major families include alpha/beta hydrolases, proteases, lipases,

esterases, and peptidases. These families are further divided into subfamilies and superfamilies based on their sequence similarity and evolutionary relationships. Serine Hydrolases are further classified into **serine proteases** (Dodson and Wlodawer, 1998) and **metabolic serine hydrolases** (Holmquist, 2000). Serine proteases include enzymes such as trypsin, chymotrypsin, and thrombin that are involved in digestion and blood clotting. On the other hand, metabolic serine hydrolases include enzymes such as acetylcholinesterase which are involved in the metabolism of neurotransmitters and other biomolecules (Long and Cravatt, 2011), and other enzymes are mentioned in the schematic

**Figure 2.** Following are some examples:

**Acetylcholinesterases (AChEs):** AChEs are SHs that hydrolyzes acetylcholine, a neurotransmitter in the nervous system. In *Drosophila*, there are two types of AChEs: Ace and Ace-related proteins.

**Carboxylesterases (CEs):** CEs are SHs that hydrolyzes carboxylic acid esters, which are common components of dietary lipids. In *Drosophila*, there are several families of CEs, including esterase-6, esterase-7, and esterase-8.

**Lipases:** Lipases are SHs that hydrolyzes triglycerides, which are stored in adipose tissue as an energy reserve. In *Drosophila*, there are several families of lipases, including Lip3, Lip4, and Lipase3-like.

**Proteases:** Proteases are SHs that hydrolyzes peptides and peptide bonds in proteins. In *Drosophila*, there are several families of proteases, including chymotrypsin-like proteases, trypsin-like proteases, and serine carboxypeptidases.

There are also several families of SHs in *Drosophila* that do not fit into the above categories, including serine peptidases with unknown function (SPU) and unclassified SHs (USHs).

It is worth noting that some SHs in *Drosophila* have multiple functions and can belong to more than one family. For example, some lipases also have esterase activity, and some proteases can also hydrolyze esters or amides.

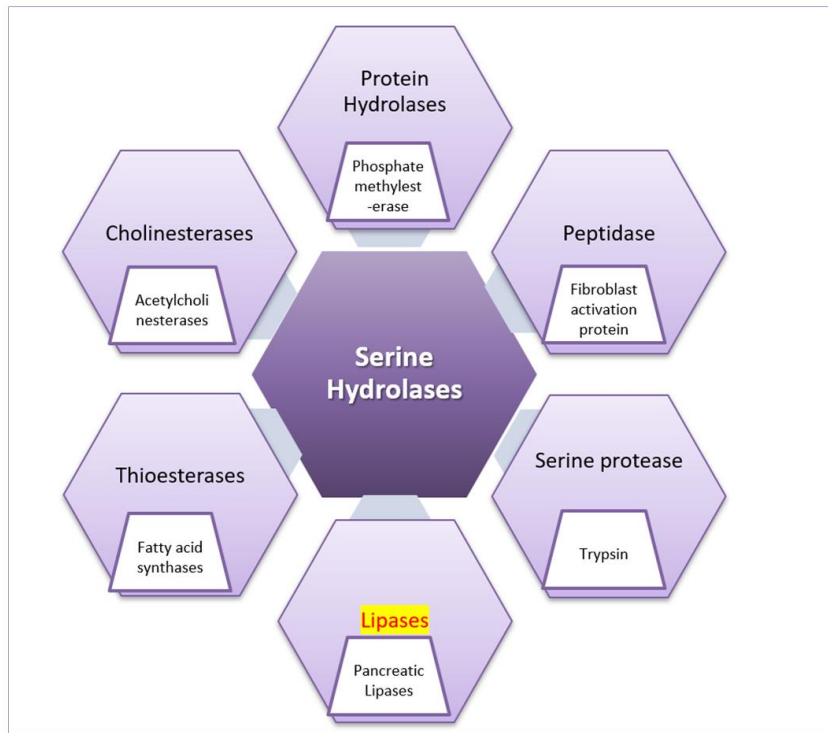


**Figure 2. Subfamilies of Serine Hydrolases.** Based on the different substrates they hydrolyze they are further classified into subfamilies. The gene CG17192 is predicted to be a lipase which is highlighted in yellow.

## Role of Metabolic Serine Hydrolases

Metabolic serine hydrolases (mSHs) are a class of enzymes that play crucial roles in lipid homeostasis, cellular metabolism, and energy balance. Recent research has pointed out how metabolic serine hydrolases play a part in controlling the immune responses of *Drosophila*.

One of the well-studied metabolic serine hydrolases in *Drosophila* immunity is Hormone-sensitive lipase (HSL) (Holmquist, 2000). HSL is expressed in the fat body, and its expression is induced upon infection with bacteria or fungi. Studies have shown that HSL plays a crucial function in the regulation of immune responses through its ability to control the levels of lipid metabolites (like triacylglycerols (TAGs), monoacylglycerols (MAGs), diacylglycerols (DAGs) and free fatty acids (FFAs)). HSL-deficient flies exhibit impaired immune responses and reduced survival upon bacterial or fungal infection, suggesting that HSL-mediated lipid metabolism is essential for mounting effective immune responses.

Another metabolic serine hydrolase involved in *Drosophila* immunity is Monoacylglycerol lipase (MGL). MGL is highly expressed in the fat body and is involved in the

hydrolysis of monoacylglycerols (MAGs), a class of lipid metabolites that are known to modulate immune responses. Studies have shown that MGL is required for the induction of AMPs and phagocytosis of bacteria by hemocytes upon bacterial infection, indicating its critical role in the regulation of immune responses.

Overall, these studies have highlighted the crucial roles of metabolic serine hydrolases in the regulation of immune responses in *Drosophila* and identified potential targets for the development of novel therapeutic strategies to combat infectious diseases.

### Lipases of Serine Hydrolases

Lipases of the SHs family are a subclass of enzymes that catalyzes the hydrolysis of ester bonds in lipids (Gupta *et al.*, 2004). They are named after the conserved nucleophilic serine residue located in their active site pocket, which plays a critical role in the catalytic mechanism.

The SHs family of lipases includes various enzymes that differ in their substrate specificity, tissue distribution, and physiological function. Some of the common types of serine hydrolase lipases include pancreatic lipase, hepatic lipase, hormone-sensitive lipase, adipose triglyceride lipase, and endothelial lipase (Mukherjee, 2003).

Pancreatic lipase serves as the principal catalyst accountable for breaking down dietary triglycerides in the small intestine. In contrast, hepatic lipase plays a role in processing lipoproteins within the liver.

HSL and Adipose triglyceride lipase are enzymes that are found in adipose tissue and play a crucial role in the regulation of lipolysis, the breakdown of reserved triglycerides into fatty acids and glycerol. Endothelial cells express an enzyme, endothelial lipase, which plays a key role in the metabolism of lipoproteins circulating in the bloodstream (Savinainen *et al.*, 2012).

Overall, lipases of the serine hydrolase family play a crucial role in lipid metabolism (as tabulated in **Figure 3**) and have diverse physiological functions in different tissues. Their catalytic mechanism and substrate specificity make them attractive targets for the development of drugs for the treatment of various metabolic disorders.



Intracellular neutral lipases	Extracellular neutral lipases	Small-molecule amidases	PLA2 superfamily
Lypolytic breakdown of neutral lipids → free fatty acids	Triglycerides/phospholipids extracellular → release of free fatty acids	Degradation of fatty acid amides	Hydrolysis of phospholipids → free fatty acid + lysophospholipid

**Figure 3. Diverse roles of Lipases.** Lipases can be classified into several categories based on their structure, source, and mode of action. Lipases can also be classified as extracellular or intracellular based on their location within the cell.

(Adapted from Berger et al., 2022)

In *Drosophila melanogaster*, lipases of the serine hydrolase family play a crucial role in lipid metabolism, which is essential for the development, survival, and reproduction of the organism. The genome of *Drosophila melanogaster* encodes for numerous serine hydrolase lipases, which are involved in the breakdown and utilization of dietary lipids, the storage and mobilization of fat reserves, and the synthesis of lipids required for membrane formation and signalling pathways.

One of the most extensively studied serine hydrolase lipases in *Drosophila melanogaster* is called Lipase 3 (Lip3), which is expressed in the midgut and is associated with the digestion of dietary lipids. Lip3 is a secreted enzyme that is synthesized as a precursor protein, which is then activated by proteolytic cleavage. Once activated, Lip3 hydrolyzes triacylglycerol molecules into fatty acids and glycerol, which are then absorbed by the midgut epithelial cells and transported to other tissues for storage or energy production.

Lipases of the serine hydrolase family play a critical role in lipid metabolism (Singh and Mukhopadhyay, 2012) in *Drosophila melanogaster*, and their functions are essential for the survival and reproduction of the organism. The study of these enzymes in *Drosophila melanogaster* has provided valuable insights into the molecular mechanisms underlying lipid metabolism and has contributed to our understanding of the regulation of energy balance and obesity in humans (Mukherjee, 2003).

### CG17192: Biodata

CG17192 is a gene of predicted lipase function located on the chromosome 3R in the *Drosophila melanogaster* (fruit fly) genome. The function of this gene is not well understood, and there is limited information available about its molecular characteristics.

Studies have shown that CG17192 is expressed in different tissues of the fruit fly, including the midgut, fat body, and carcass, suggesting that it may have a role in various physiological processes (refer to **Table 1**).

The gene is predicted to span a region of approximately 1.5 kb and contains two exons and two introns. The CG17192 gene model predicts that the transcript encodes a protein of 337 amino acids in length (1-16 a.a. spans signal peptide, 36-337 a.a. encodes for the Pfam Lipase). However, the function of this protein is not well understood.

	Characteristic	Description	
1.	Gene Location	3R:27,017,180..27,018,287 [-]	
2.	Expression pattern	Tissues	midgut, carcass, fat body
		Development	adult male and female
3.	Molecular weight	37kDa	
4.	Length of the protein	337 a.a.	
		1052 nucleotides	
5.	Localization	Extracellular region	
6.	Molecular/Biological function	Lipid Catabolic process	
7.	Orthologs (Similarity)	PLA1A (50%), LipH (45%), LipC (44%)	
8.	Homologs	CG17191, CG6295, CG6283	

**Table 1. Gene Report describing Characteristic features of CG17192 obtained from [FLYBASE](#).** The table highlights important characteristics of the gene, including its chromosomal location, molecular function, and biological processes involved.

Expression studies have shown that CG17192 is expressed at low to moderate levels in an adult male and female stages.

Despite its unknown function, CG17192 has been implicated in various studies. For instance, a genome-wide association study (GWAS) has identified a potential association between CG17192 and Lipid metabolism in *Drosophila*, suggesting that the gene may have a role in regulating lipid metabolic activity. Additionally, a transcriptome analysis of aging flies has shown that CG17192 expression is altered in older flies compared to young ones (in the adult male), while the opposite is observed in adult female flies, indicating a potential involvement in the aging process.

Further research is needed to fully understand the function of CG17192 and its potential role in development, disease, or other biological processes.

## Regulation of Dietary Lipid Uptake via CG17192: An Insight into the Molecular Mechanisms

A previous report focuses on the role of the E78 nuclear receptor in regulating lipid metabolism in *Drosophila* (Praggastis *et al.*, 2021). The study found that the E78 nuclear receptor is a key regulator of dietary triglyceride uptake and systemic lipid levels in *Drosophila*. The researchers used genetic manipulations to demonstrate that loss of E78 function led to an increase in circulating triglycerides, while overexpression of E78 resulted in decreased triglyceride levels.

One of the genes that was identified as being regulated by E78 is CG17192, which is predicted to encode a protein with an unknown function. The study showed that CG17192 is upregulated in response to dietary triglycerides and that its expression is dependent on E78. The researchers hypothesized that CG17192 may play a crucial role in lipid metabolism (as shown in the model, **Figure 4**), and further studies will be necessary to determine its precise function. Overall, the study highlights the importance of the E78 nuclear receptor in regulating lipid homeostasis in *Drosophila* and identifies CG17192 as a potential target for further investigation in this context.

The article provides evidence that lipid metabolism is transcriptionally regulated by the E78A nuclear receptor through the expression of a digestive lipase gene, CG17192, which is a previously uncharacterized lipase in *Drosophila*. According to the findings of this study, CG17192 plays a crucial role in breaking down and absorbing approximately 30% of dietary triglycerides in adult *Drosophila*. The E78A receptor specifically functions within the intestine to control this lipase's transcription and regulate whole-body lipid homeostasis.

Further research on the role of CG17192 in lipid metabolism could have significant implications for understanding and treating metabolic disorders, such as obesity and diabetes.

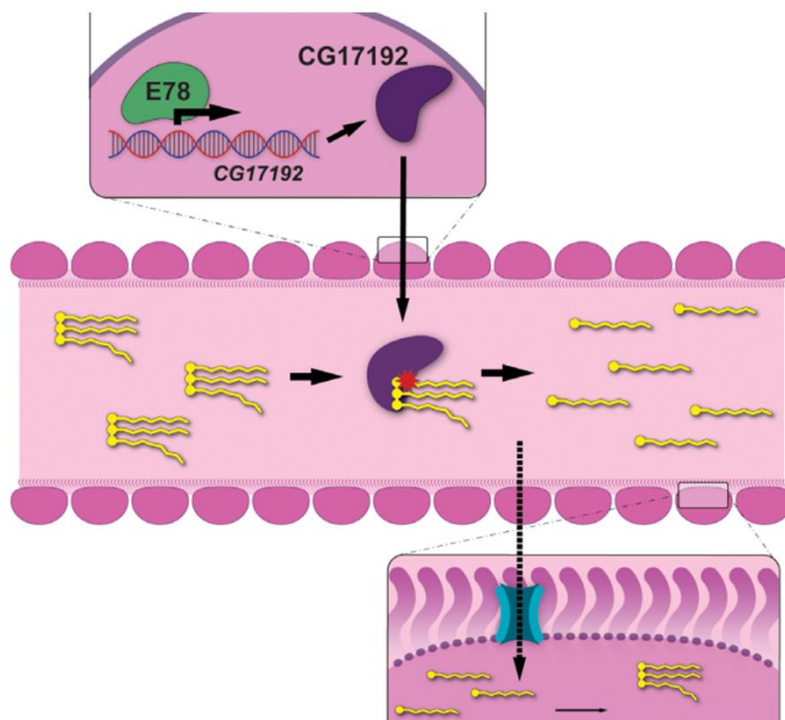


**Figure 4. Regulatory mechanism of E78A in controlling the uptake of dietary lipids through CG17192.** The lipase CG17192, which is produced specifically in the intestine, is regulated by E78A at the transcriptional level. Once produced, CG17192 is secreted into the intestinal lumen where it breaks down dietary triglycerides (TGs) into free fatty acids (FFAs). These fatty acids can then be taken up by the enterocytes. Once inside, the FAs are re-esterified into triglycerides and diacylglycerides that can be utilized as a source of energy or transported to other tissues in the fly.

(Adapted from Praggastis et al., 2021)

### Serine Hydrolases: Key Players in Immune Defense Mechanisms

Serine hydrolases are a diverse class of enzymes that are involved in many biological processes, including immunity. They are involved in the regulation of immune responses and are critical for the proper functioning of the immune system.

In addition, some serine hydrolases are involved in the regulation of T-cell responses. For example, one serine hydrolase, called diacylglycerol lipase (DAGL), is involved in the production of 2-arachidonoylglycerol (2-AG), a lipid mediator that is associated with the regulation of T cell function. By modulating the levels of 2-AG, DAGL helps to regulate T-cell responses and maintain immune homeostasis (Poursharifi *et al.*, 2017). Serine hydrolases are also involved in the metabolism of endocannabinoids, which are lipid molecules that have immunomodulatory effects. These enzymes are associated with the breakdown of lipid mediators that are produced during inflammation, such as prostaglandins (Dinh *et al.*, 2002). By regulating the levels of endocannabinoids, serine hydrolases help to regulate immune responses and maintain immune homeostasis.

Overall, the role of serine hydrolases in immunity is complex and multifaceted. These

enzymes play important roles in regulating immune responses, and their dysfunction can contribute to the development of immune-related diseases.

## Innate Immunity in *Drosophila*

*Drosophila melanogaster*, commonly known as fruit flies, have a well-developed immune system that defends them against a wide range of pathogens. The immune response of the *Drosophila* is mostly hemocyte mediated (see

**Figure 5.)** (Lemaitre and Hoffmann, 2007). The immune system of fruit flies comprises both cellular and humoral responses.

### Cellular responses

**Phagocytosis:** Fruit flies have specialized immune cells called hemocytes, which engulf and destroy invading pathogens by phagocytosis.

**Melanization:** In response to certain pathogens, hemocytes secrete a cascade of enzymes that convert tyrosine into melanin, a dark pigment that surrounds and kills the invading pathogen (Lemaitre and Hoffmann, 2007).

**Encapsulation:** Hemocytes can also form a physical barrier around large pathogens, such as parasitic wasps, preventing their growth and spread.

### Humoral responses

**Antimicrobial peptides (AMPs):** Fruit flies produce a variety of AMPs in response to bacterial and fungal infections. AMPs can directly kill or inhibit the growth of pathogens (Lemaitre and Hoffmann, 2007).

**Reactive oxygen species (ROS):** Fruit flies also produce ROS, which have antimicrobial properties and can damage the DNA and proteins of pathogens.

**RNA interference (RNAi):** Fruit flies have a sophisticated RNAi mechanism that can recognize and destroy viral RNA, preventing viral replication.

Overall, the *Drosophila* immune system is capable of responding to a wide range of pathogens, including viruses, parasitic wasps, fungi, and bacteria. The combination of cellular and humoral responses provides an effective defense against pathogens and helps ensure the survival of fruit flies in their natural environment.

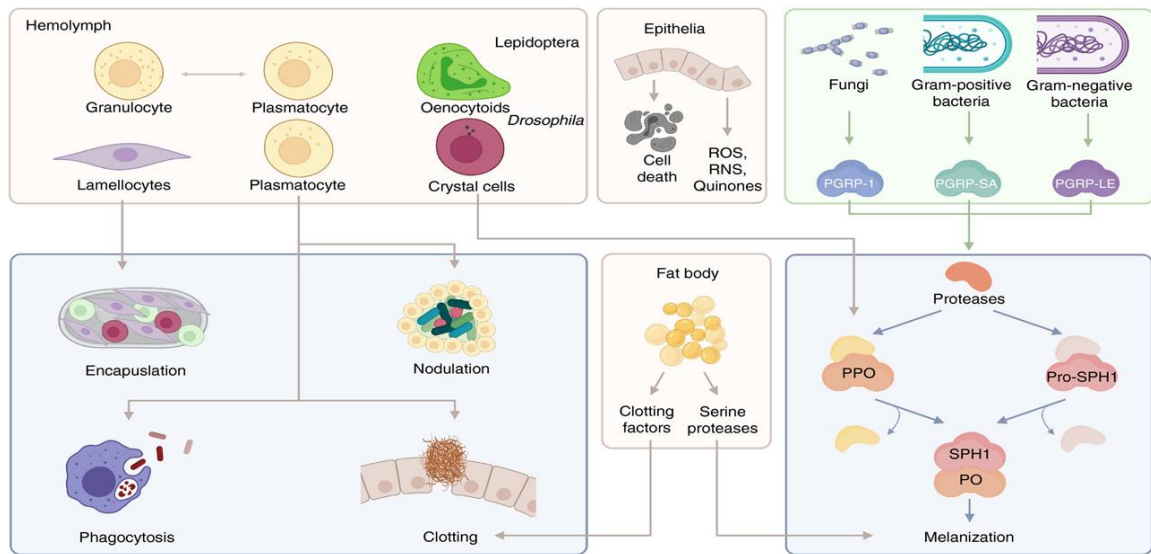


**Figure 5. Haemocyte-mediated immunity in insects:** This diagram depicts the crucial role of haemocytes in defending against pathogens and parasites as well as promoting wound healing. The figure showcases diverse types of haemocytes, comprising plasmatocytes, lamellocytes, oenocytoids/crystal cells, and granulocytes, along with their reactions to microbial or parasitic invasion. These responses involve encapsulation by lamellocytes, phagocytosis, hemolymph clotting, nodulation via plasmatocytes, and melanization through oenocytoids and crystal cells. Additionally demonstrated are the involvement of both haemocyte populations alongside the fat body during prophenoloxidase (PPO) cascade activation along with epithelial contribution to immunity that is represented by cytotoxic species like Reactive Nitrogen Species (RNS), Reactive Oxygen Species (ROS), and quinones present within it. Furthermore, the illustration exhibits how the adipose tissue instigates the generation of coagulation factors and serine proteases in response to infection, which governs the process of melanization. The identification of microorganisms stimulates peptidoglycan recognition protein (PGRP) expression, responsible for managing protease activity that modulates melanization reaction and PPO cascade.

(Adapted from Eleftherianos et al., 2021)

## Serine Hydrolase in *Drosophila* Immunity

SHs also play a critical role in the immune system of *Drosophila*, which is a widely used model organism for studying innate immunity.

In *Drosophila*, serine hydrolases are involved in the regulation of antimicrobial peptide (AMP) production (Lemaitre and Hoffmann, 2007). AMPs are small peptides that are produced by the immune system in response to infection, and they play an important role in fighting off pathogens.

One of the main roles of serine hydrolases in the *Drosophila* immune responses is in the regulation of the Toll pathway, which is one of the major signalling pathways involved in the innate immune response. The Toll pathway gets activated in response to infection and triggers the synthesis of antimicrobial peptides (AMPs), which can kill

invading pathogens (Valanne *et al.*, 2011).

Studies have shown that serine hydrolases play a critical role in the regulation of the Toll pathway. Serine hydrolases have been shown to be required for the synthesis of AMPs in response to infection. These Hydrolases regulate the production of a lipid molecule called diacylglycerol (DAG), which is essential for the toll pathway activation. Overall, serine hydrolases play a critical role in the regulation of the innate immune response in *Drosophila*. Dysfunction of these enzymes can lead to impaired immune function and increased susceptibility to infection.

### CG17192 in *Drosophila's* immunity

CG17192 is an orphan serine hydrolase which is predicted to be involved in *Drosophila's* immunity. The negative log FC value (in **Table 2.**) represents that the gene is getting downregulated with respect to the infection tabulated below:

Gene Symbol	Pathogen type	Infection	Log FC value	Developmental stage	References
CG17192	Fungus	Aspergillus fumigatus	-0.27	Adult	(De Gregorio <i>et al.</i> , 2002)
	Bacteria	E. coli, M. luteus	-1.13	Adult	(De Gregorio <i>et al.</i> , 2001)
	Bacteria	Pseudomonas entomophila	-1.149329102	Adult	(Ragheb <i>et al.</i> , 2017)
			-0.7935	Adult	(Soory and Ratnaparkhi, 2022)
	Virus	Sindbis Virus	-0.9785	Adult	(Waring <i>et al.</i> , 2022)
	Fungus	Beauveria bassiana	-0.81	Adult	(Paparazzo <i>et al.</i> , 2013)

**Table 2. Summary of CG17192 Gene Downregulation in Response to Various Infections, with Corresponding References**

This downregulation of gene expression results in immune suppression, which can make the host more susceptible to infection. Therefore, understanding the specific mechanisms of immune suppression and identifying key genes involved in regulating the immune response can lead to the development of more effective therapies for combating immunodeficiencies and infectious diseases. This knowledge can also aid in the development of new vaccines, drugs, and immunotherapeutics that may enhance immune function and prevent serious infections. It is imperative that researchers continue to investigate immune suppression and explore potential treatments, as immunodeficiency and infectious diseases remain a major global health concern.

# Chapter 2 Materials and Methods

## SLiCE (seamless ligation cloning extract) based Cloning strategy

The SLiCE-based approach was used for cloning the gene of interest in the vectors (pET45b+ and pRM). The SLiCE method involves three crucial steps:

**Preparation of the DNA fragments to be cloned:** The DNA fragments to be cloned are amplified using PCR and purified. The PCR primers used to amplify the fragments contain additional sequences that are homologous to the cloning vector.

**Preparation of the cloning vector:** The cloning vector is prepared by linearizing it with a restriction enzyme that cuts only once in the vector sequence.

**Transformation and selection:** The linearized vector and the PCR-amplified DNA fragments are mixed together and transformed into competent cells. The selection of cells is determined by their capacity to thrive in the vector's exclusive antibiotic environment. The resulting colonies should contain the cloned DNA fragment inserted into the vector sequence.

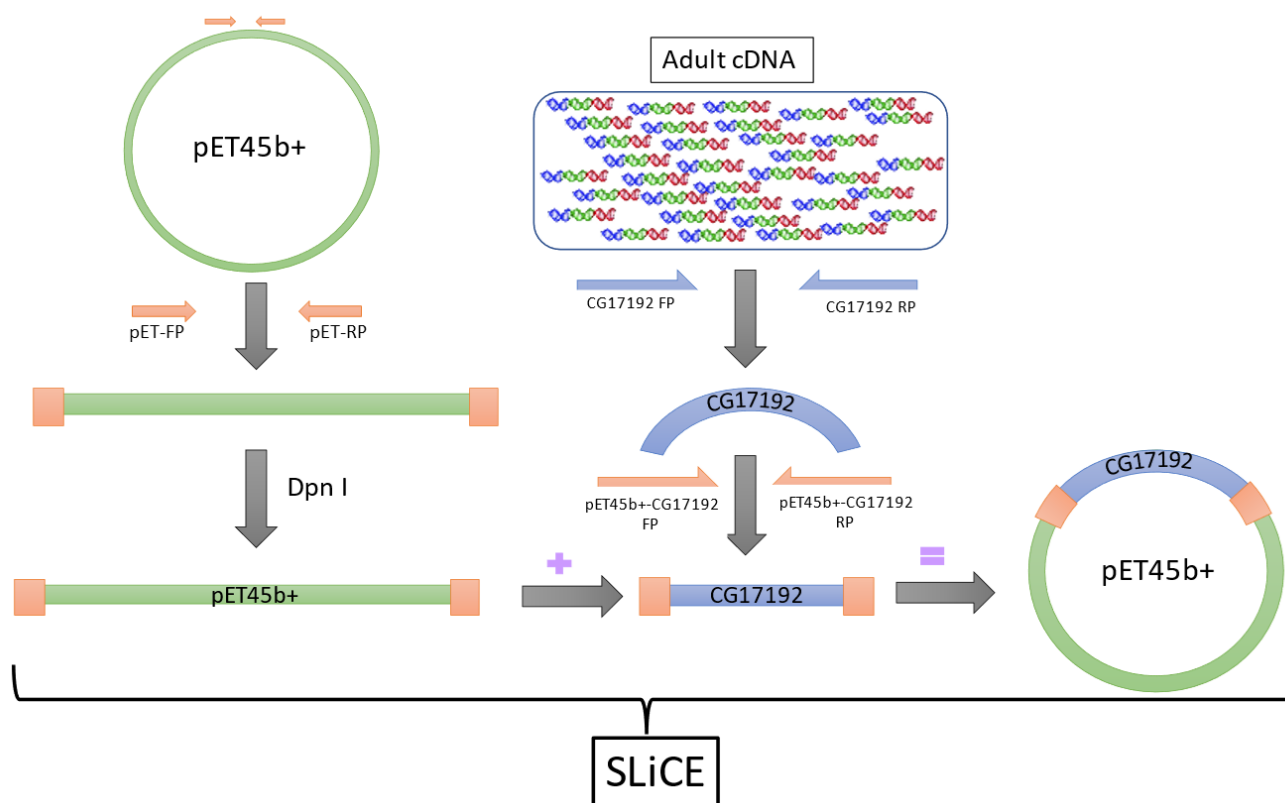


**Figure 6. Schematic of clone designed by SLiCE(seamless ligation cloning extract) based approach**

Here green circle represents the vector (pET45b+, pRM) with 2 (pET45b+, pRM) primers whereas Blue color represents CG17192 (Gene of interest), the orange color denotes similar 10-15 bp in both the vector and the insert. '+' sign indicates transformation of the vector and insert in the competent cells (PPY) and '=' indicates the positive recombinant plasmid



## Oligos Designed for Cloning

The primers for inserting the gene CG17192 in the bacterial expression vector, pET45b+, with a His-tag at its N terminus, were designed using the snapgene tool. The N-terminal of the forward primer consists of 6x His overhangs (as highlighted in the table), while the C-terminus has overhangs of the vector sequences. The PCR amplification of the vector pET45b+ was done using forward & Reverse primers (as mentioned in **Table 3**).

For the Cloning of the gene CG17192 in the bacterial expression vector, pET45b+ with a His-tag at its N terminus, CG17192 was PCR amplified using the pool of adult cDNA of *Drosophila melanogaster* using the primers (refer to **Table 3**). To optimize the annealing temperature for the primers, gradient PCR was done.

For making the enzyme catalytically dead, the mutation was made at the 179<sup>th</sup> from serine to alanine of the gene CG17192 in pET45b+, in which two-step PCR was applied to mutate it successfully. A two-step PCR way was approached to make a mutation at the 179<sup>th</sup> position.

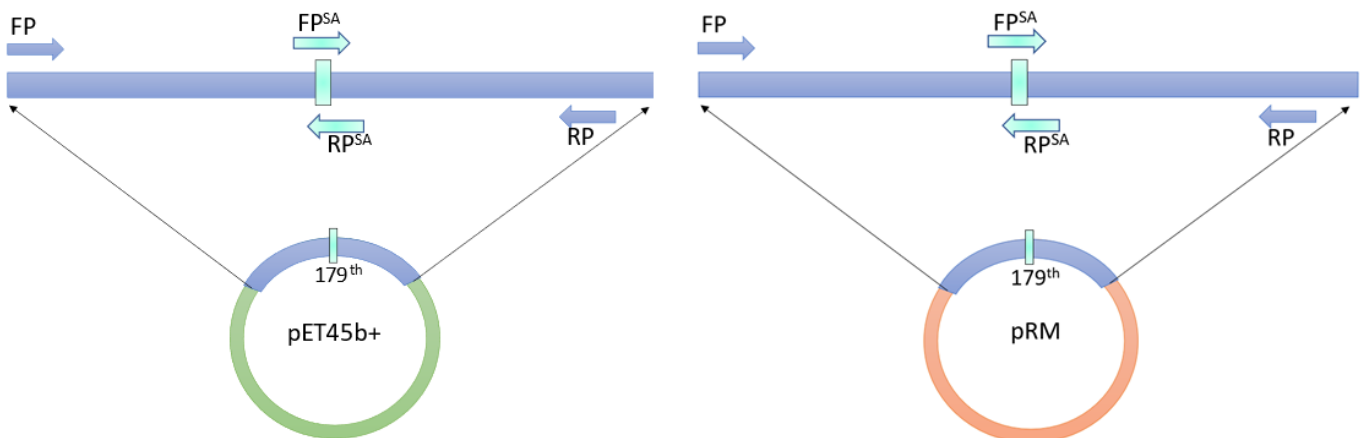


**Figure 7. Site Directed mutagenesis using SLiCE based approach for cloning.** In this image, FP and RP represent forward and reverse primer respectively (common for the vector and gene of insert). While, Fp<sup>SA</sup> and RPs<sup>SA</sup> represent mutation at 179<sup>th</sup> amino acid of the insert in which serine (AGT) is mutated to alanine (GCC). Cyan color shows the mutated site at the gene of interest. Green circle represents the vector (pET45b+ and pRM) and blue segment represents CG17192 (Gene of interest)

First step PCR was done using primers pET45b+-6xHis-CG17192 FP and pET45b+-6xHis-CG17192 <sup>S179A</sup> RP. The other set consists of pET45b+-6xHis-CG17192 RP and pET45b+-6xHis-CG17192 <sup>S179A</sup> FP in which CG17192 was used as a template for amplification that made a mutation at 179<sup>th</sup> position from Serine to alanine.

For the latter step, PCR was set up in such a way that the templates from the first PCR were used for it. The primers used in this case were pET45b+-6xHis-CG17192 FP and pET45b+-6xHis-CG17192 RP, which resulted in a mutation. (refer to schematic **Figure 7**). Further, these were transformed in PPY cells with pET45b+ using the SLiCE method. PCR screening was done for positive colonies, and to validate its insertion, sanger sequencing was done.

### For Optimizing protein expression by pruning a start codon at the N terminus

For removing an extra start codon before the His tag, the primers were designed, which are tabulated in **Table 3**. SLiCE-based cloning was used, which consists of 10-15 homologous bases as that of the vector. Here, the templates used were the plasmids obtained after amplifying with the primers of sr. no. 2 and 3 (from **Table 3**) through PCR.

Sr. no.	Plasmids		Primers
1.	pET45b+	Forward Primers	gtgggtaccggttcgaatga
		Reverse Primers	gtgatggtggtggtgatgtg
2.	pET45b+-6x His-CG17192	Forward Primers	cacatcaccaccacatcacatgagggagtatttttctagcagc
		Reverse Primers	tcattcgaaccggtaccacattcagttgcccgaatggag
3.	pET45b+-6x His-CG17192 <sup>S179A</sup>	Forward Primers	tgattggacatgccttgggtgcccatgtg
		Reverse Primers	tgggcaccaaggcatgtccaatcacctc
4.	pET45b+-6x His-CG17192 & pET45b+-6x His-CG17192 <sup>S179A</sup> Pruning 1 ATG	Forward Primers	atggcacatcaccaccacatcacggaggcagggagtattttt
		Reverse Primers	gcctccgtgatggtggtgatgtgccat

**Table 3. Primer sequences designed for insertion and site-directed mutagenesis of CG17192 in the bacterial expression vector, pET45b+**

The cloning strategy used was SLiCE (Seamless Ligation Cloning Extract). It is a method for cloning DNA fragments into a vector using homologous recombination. It allows for the efficient and seamless insertion of DNA fragments without the need for restriction enzymes, ligases, or PCR amplification.

## Cloning of the gene CG17192 in the insect expression vector pRM

For Cloning of the gene CG17192 in the insect expression vector, pRM with a His-tag at its N-terminus, SLiCE-based cloning was used, which consists of 20 homologous bases (see **Table 4.**) as that of the vector.

For Cloning of the gene CG17192 in the insect expression vector, pRM with a FLAG tag at its C terminus, SLiCE-based cloning was used, which consists of 10-15 homologous bases as that of the vector. First, the FLAG tag was inserted at the C terminus of the gene CG17192 using Reverse Primer, while Reverse primer 2 was used to clone CG17192-FLAG in pRM.

The primer sequence used for this cloning is tabulated below:

Sr. no.	Plasmids		Primers
1.	pRM	Forward Primers	ggatcctctagagtcgacctgc
		Reverse Primers	gtgatgggtgggtgatgcatggtaccgagctcgaattc
2.	pRM-6x His-CG17192	Forward Primers	catcaccaccaccatcacatgagggagttatcttagcagc
		Reverse Primers	ctctagaggatccctattcagttgcccgaatggag
3.	pRM-6x His-CG17192 <sub>S179A</sub>	Forward Primers	tgattggacatgccttgggtgcccatgtg
		Reverse Primers	tgggcacccaaggcatgtccaatcacctc
4.	pRM-CG17192-1x FLAG	Forward Primers	gaattcgagctcggtagcatgagggagttatcttagcagc
		Reverse Primers-1	cttatcatcatcatccttgaatcttcagttgcccgaatg
		Reverse Primers-2	caggctgactctagaggatccctacttatcatcatcatcctt-gtaatc
5.	pRM-CG17192 <sub>S179A</sub> -1x FLAG	Forward Primers	tgattggacatgccttgggtgcccatgtg
		Reverse Primers	tgggcacccaaggcatgtccaatcacctc

**Table 4** Primer sequences designed for insertion and site-directed mutagenesis of CG17192 in the insect expression vector, pRM.

The Bio-rad thermocycler utilized the following components (see **Table 5.** and **Table 6**) in order to carry out gene amplification.

	Reagents	Volume (μl)
1.	Nuclease Free water	39
2.	10x Hi buffer	5
3.	10mM dNTPs	2
4.	Primers (FP)	1
5.	Primers (RP)	1
6.	Polymerase	1
7.	Template(100ng/ul)	2

**Table 5. PCR reaction volumes are depicted in microliters (μL) for a typical 50 μL reaction, including template DNA, primers, nucleotides, and polymerase.**

	Denaturation		Annealing	Elongation	
Temp (C)	95 °C		60 °C	72 °C	
Time (min)	2:00 min	00:20 min	00:20 min	02:45 min	10:00 min

**Table 6. PCR temperature profile showing the three main steps:** initial denaturation at a high temperature, followed by annealing at a lower temperature, and extension at an intermediate temperature, with the optimal temperatures depending on the specific primers and DNA template used.

The amplified DNA samples were subjected to electrophoresis on a 0.8% Agarose gel to confirm the presence of the intended gene bands. Subsequently, the PCR Purification Kit from Qiagen was utilized to isolate and purify the amplified DNA from the PCR products.

### Transfection in Insect derived cells

Full-length CG17192 and CG17192<sup>S179A</sup> were cloned in pRM vector with N-terminal His and aC-terminal FLAG tag at its C terminus & ampicillin antibiotic resistance. Catalytically inactive S179A CG17192 (serine residue at 179th position was changed to alanine) was generated using whole plasmid PCR and SLiCE-based cloning.

S2 cells that were transiently stably transfected with the plasmid pRM-His-CG17192, pRM--His CG17192<sup>S179A</sup>, pRM-CG17192-FLAG, and pRM-CG17192<sup>S179A</sup>-FLAG. These transfected cells were harvested and preserved in Gibco Schneider's Drosophila medium (Thermo-fisher scientific, #21720024) along with 10% fetal bovine serum (Thermo-Fischer scientific, #10082147) that had been heat-inactivated. The temperature was maintained at 23°C, and the cells were passed once every 3-4 days. After 20 passages, the cells were discarded. For our transfections, we used 70-80% confluent cells in 6 well flasks, and the volume was set to 1 mL. We used TransIT-Insect Transfection Reagent (Mirus, #6100) to transfect 2μg of plasmid, following the

manufacturer's protocol. As a control, we transfected the mock cells with an empty vector using the same procedure. The transfected cells were later induced with 0.5 mM CuSO<sub>4</sub> 2 hours post-transfection, and they were allowed to grow until they achieved 100% confluency (for around 48 hours).

For harvesting the cells, Cells were pipetted into a 1mL tube, and the collected cells were pelleted using centrifugation at 1000\*rcf at 18 °C. And the cell pellet, supernatant, and culture media were separated and were flash freeze to be stored at in -80 °C. The transfected cells were thawed on ice and resuspended in 100 µL of 1xPBS (phosphate buffer saline) solution. The cells were lysed by probe sonication for 5 seconds with 1 second on and 1 second off pulse at an amplitude of 60%. The lysed cells were ultra-centrifuged at 4 °C for 45 minutes at a speed of 21,000 \* g. The supernatant was collected in an Eppendorf, while the membrane pellet was resuspended in 100 µL of PBS and sonicated for 5 seconds, 1 on 1 off, till the pellet gets solubilised. Expression and activity check for the cells were done using western blotting and Activity Based Protein Profiling (ABPP), respectively. Protein estimation using a BCA kit was done, and each sample was diluted to 5mg/ml concentration for a volume of 100 mL.

## Transformation and Protein Expression

Plasmids were transformed, and their protein expression was validated in BL21-De3 and BL21-Rossetta cells.

Primary culture of 5-10ml of LB (Lysogeny broth) was set from the glycerol stocks of pET-His-CG17192 and pET-His-CG17192<sup>S179A</sup> 37°C for overnight 12-14 hours. Secondary cultures were set from the primary culture, and protein expression was induced with IPTG (0.5mM) at 18°C for 16 hours.

Bacterial cells were centrifuged at 6800\*g rcf for 10 min at 4 °C. The resulting supernatant was discarded, and the pellet was resuspended in 100 µL chilled sterile 1x PBS of pH 7.4. Cells were lysed by Sonication for 10 min (Pulse: 10 sec ON; 10 sec OFF) on ice. Lysed cells were centrifuged at 15000\*g for 30 minutes at 4°C, and the resulting supernatant (termed “soluble proteome”) and the pellet (termed “pellet proteome”) were collected in different eppendorfs. For the gel-based ABPP assays, 50 µL of a 1 mg/mL solution was treated with FP-Rhodamine (concentration: 2 µM, time: 45 min, temp: 37 °C, with the shaking of 750 rpm) (FP-Rhodamine was Borrowed from Dr. Siddhesh Kamat which was synthesized via the protocol reported in an article (Liu et al., 1999)). To terminate the reaction, 12.5 µL of 5x SDS loading buffer was added and

subsequently subjected to boiling (at a temperature of 95 °C for a duration of 10 minutes). The proteomes labeled with fluorescence were separated using SDS-PAGE gel, which has a composition of about 10%. A Syngene G-Box Chemi-XRQ system meant for documentation was employed in visualizing these samples.

### **Protein estimation using BCA (Bicinchoninic Acid)**

The BCA protein assay kit (Thermo-Fischer Scientific, #23225) was utilized to estimate the concentration of protein by comparing it with known standards. To perform the estimation, 2.5 µL of protein was mixed with 100 µL of the BCA reagent, resulting in a 5x dilution, and then incubated in a 96-well plate at 37 °C for 30 minutes. The absorbance of the resulting solution was measured at 562 nm using a Varioskan Flash (Thermo-Fischer Scientific, #LS-0809-0331). Following the estimation process, the final samples were prepared at a concentration of 1 mg/mL by adding 1xPBS buffer at a pH of 7.5.

### **Gel-based ABPP: A Powerful Technique for qualitative analysis of serine hydrolases**

ABPP has been particularly useful in studying serine hydrolases, as it allows for the identification and characterization of active enzymes in complex biological systems (Liu *et al.*, 1999).

One of the most commonly used probes for studying serine hydrolases is the fluorophosphonate (FP) probe (Simon and Cravatt, 2010). This probe contains a serine-reactive group that covalently binds to the active site serine residue of serine hydrolases, as well as a fluorescent tag that allows for visualization and quantification of labeled proteins. FP probes have been used to profile serine hydrolase activity in a variety of systems, including whole cells, tissues, and organisms. The application of activity-based protein profiling (ABPP) utilizing fluorophosphonate probes has yielded novel insights into the functions of serine hydrolases in numerous biological processes. One area of study pertains to lipid metabolism, encompassing triglyceride hydrolysis and endocannabinoid synthesis. Additionally, ABPP offers promising prospects for identifying new therapeutic targets with regard to illnesses like cancer, obesity, and neurodegenerative disorders.

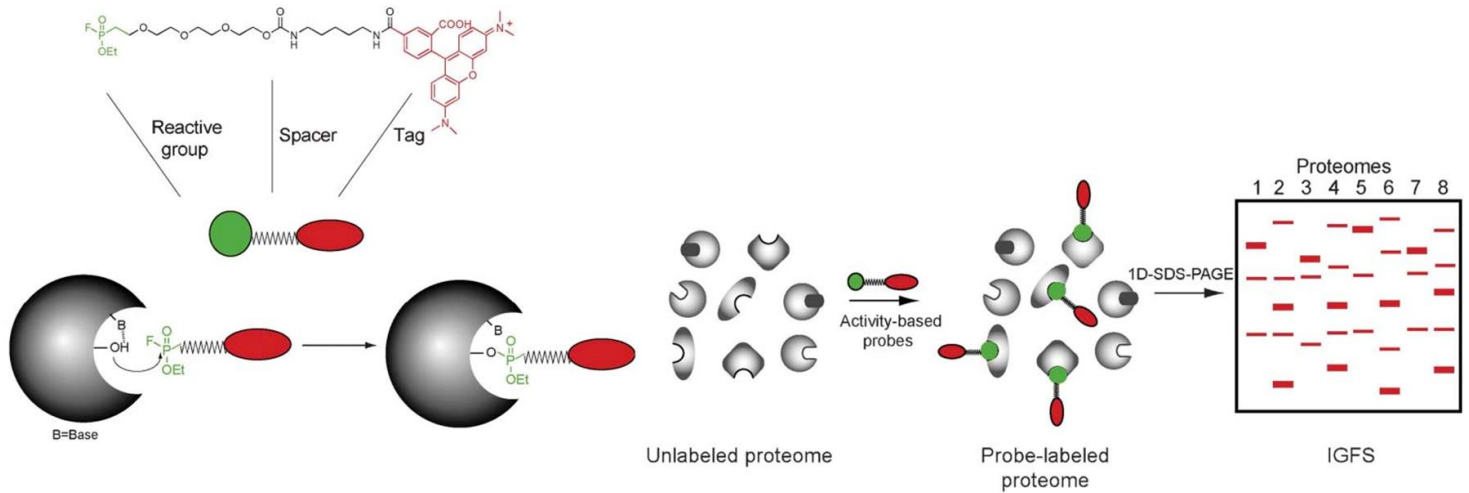


**Figure 8. ABPP probes targeting the SH enzyme family.** The ABPP probes are designed to target the SH enzyme family and are made up of three components: a reactive warhead, a spacer, and a reporter tag like Rhodamine. When using fluorophosphonate (FP) probes, the reactive group modifies the active site serine nucleophile of SHs in a covalent manner. The results of ABPP experiments are analyzed using in-gel fluorescence scanning (IGFS), where proteomes are treated with the ABPP probes that are conjugated with a fluorophore. The enzymes labeled with the probes are then separated using SDS-PAGE and can be visualized using IGFS. The figure illustrates both active and inactive enzymes, which are represented by open and blocked active sites, respectively.

Adapted from (Sieber and Cravatt, 2006)

This technique possesses the capacity to facilitate drug development efforts that can ultimately result in innovative therapeutics for a range of ailments.

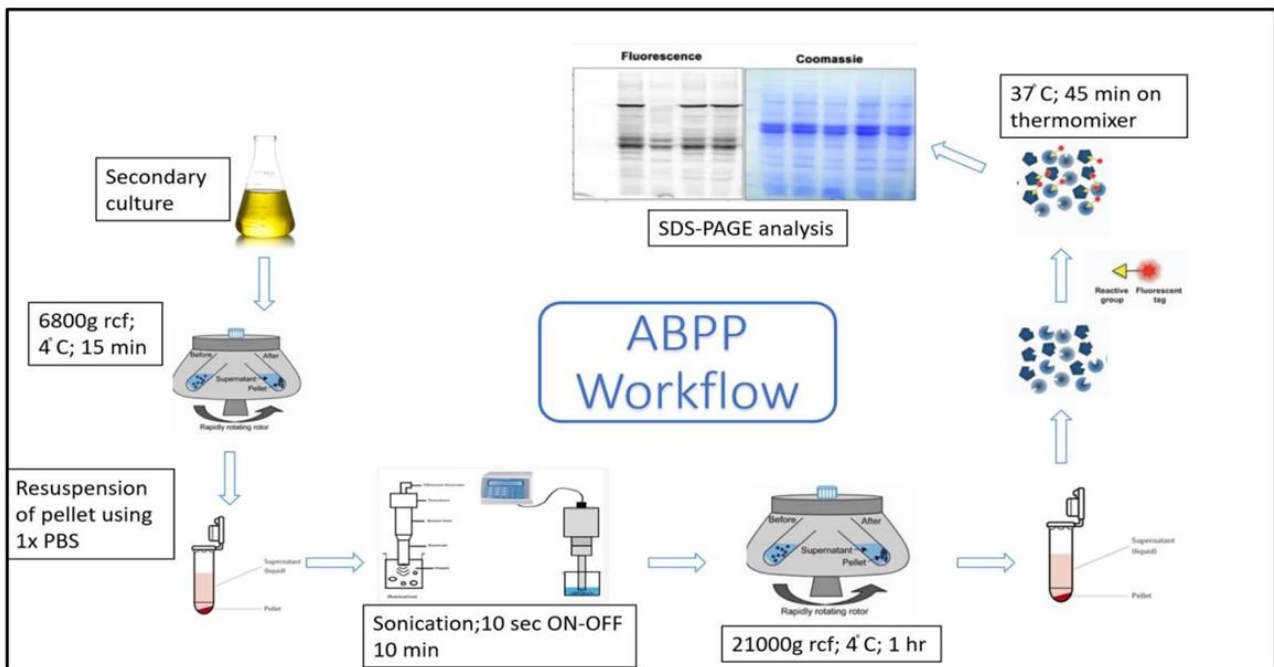


**Figure 9. Schematic of the Activity based protein profiling (ABPP) workflow for bacterial lysates**

## Sample Preparation and Analysis of ABPP and Western Blot Techniques

For expression check, samples were run on a resolved 10% (and sometimes 12%) SDS PAGE gel and transferred to a PVDF (polyvinylidene fluoride) membrane in 1x transfer buffer for 90 min at 4 °C at a constant voltage of 90V. After transfer, the membrane was blocked for around 1 hour in 5% (w/v) milk in TBST (0.1% (w/v) Tween) (phosphate buffered saline with tween 20) and then probed overnight with primary antibody, anti-FLAG mouse in 1:5000 dilution. The membrane was washed thrice in TBST and incubated in anti-Mouse HRP secondary antibody at a dilution of 1:10,000 for an hour at room temperature (RT). The membrane was washed again in PBST three times, and a blot was developed using an HRP-sensitive chemiluminescent substrate and imaged in G-Box. The blot was stripped and reprobed for GAPDH as the loading control with anti-tubulin in 1:5000 dilution. For activity check, gel-based activity profiling was done. Membrane proteomes (for mock and WT CG17192 cells) were incubated with 2  $\mu$ M of FP-Rhodamine (Fluorophosphonate fluorophore) and incubated at 37°C at 750 rpm for 45 minutes and then quenched with 5X loading dye (25  $\mu$ L of 5X loading dye for 100  $\mu$ L of the sample) and boiled at 95°C for 10 minutes and loaded on to a 10% SDS PAGE. The activity gel is imaged using a Syngene G-Box.

## Protein Purification under native condition

The recipe for the preparation (Rajendran *et al.*, 2020) of the Native Lysis Buffer (50mM Tris-Cl; 5% glycerol; 10mM Imidazole), Native washing Buffer (50mM Tris-Cl; 5% Glycerol; 20mM Imidazole or 40mM Imidazole or 60mM Imidazole), and Native Elution Buffer (50mM Tris-Cl; 5% Glycerol; 200mM Imidazole or 400mM Imidazole or 500mM Imidazole) was as mentioned. Harvest cells from a 50 mL culture by centrifuging at 6800\*g rcf for 15 minutes at 4°C, then resuspend them in 8 mL of Native Binding Buffer. Sonicate for 10 minutes with a 10-second pulse on and a 10-second pulse off. After centrifuging at 6800\*g for 10 minutes to remove cellular debris, transfer the supernatant to a new tube and save 50 $\mu$ L of the lysate for SDS-PAGE analysis. Allow Ni-NTA agarose beads to bind for 2-3 hours with gentle agitation. Settle the resin using low-speed centrifugation (500\*g), then remove the supernatant and save 50 $\mu$ L for SDS-PAGE analysis at 4°C. Repeat the washing step thrice with 1 mL of Wash Buffer each time (consecutively with increasing imidazole concentration). Elute the protein with 200  $\mu$ L of Native Elution Buffer and keep the supernatant at 4°C for SDS-PAGE analysis. Repeat this elution step three more times, collecting 50 $\mu$ L fractions each time for analysis and snap-freezing the rest of the 150  $\mu$ L in another tube.



## Fly Husbandry and Lines

The species, *Drosophila melanogaster* (for fly lines, refer to **Table 7.**), was grown on a standard cornmeal agar medium and was maintained at a temperature of 25°C.

Sr. no.	Line (Genotype)	Source	Description	Chromosome location
1.	CG17192RNAi (UAS-CG17192 <sup>RNAi</sup> )	BDSC	BDSC: 56042	2L
2.	NP-1 Gal4 (Myo-81F <sup>ts</sup> )	BDSC	BDSC: 67067	2L

**Table 7.** Fly lines with genetic mutations describing their respective source, stock number, and chromosomal location.

## Bacterial Clearance Test

In this study, UAS-CG17192i was crossed with NP1-Gal4 (Myo-81F<sup>ts</sup>), and the offspring (NP1-Gal4>UAS-CG17192i) were used for further experimentation. *Pseudomonas entomophila* (P.e) is used in this study. To test the resistance of the pathogen to rifampicin (100ug/ml) and its ability to hydrolyze casein on a milk agar plate, a bacterial strain was chosen. The pathogen was cultured overnight in a broth, and the resulting bacterial pellet was dissolved in a 5% sucrose solution to obtain a final OD<sub>600</sub> of 200. For all the bacterial clearance assays (for the workflow, refer to **Figure 10.**), female flies aged between 6-8 days were subjected to a period of food and water deprivation for two hours. Following this, the flies were transferred onto a filter disk that had been dipped in the concentrated bacterial solution, where they were fed for an experimentally determined duration. To evaluate bacterial clearance efficacy, the flies were then placed into vials containing standard fly food at densities of 7-8 per vial, and their ability to clear bacteria was measured after time points of both 0 hours post-infection (hpi) and 6 hpi.

To evaluate the bacterial burden, *P. ent* was provided to flies for a duration of 2 hours. Afterward, these insects underwent surface sterilization using 70% ethanol for half a minute and were permitted to air-dry. The entire fly specimen was then crushed in 100 LB before plating the lysate onto an agar plate containing rifampicin for bacterial assessment at 0 and 6 hours post-infection (hpi).

On crossing UAS-CG17192i with Fat-Body Gal4 (FB-Gal4) (P{GAL4}fat), 5–10-day old female adult flies of FB-gal4>UAS-CG17192i (F1 offspring) were eventually infected

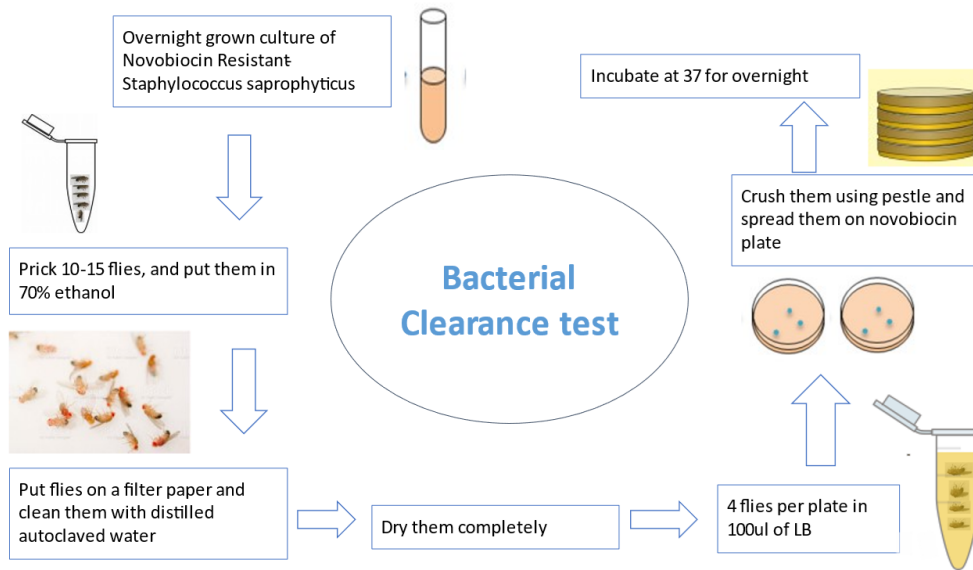


Figure 10. Workflow of Bacterial Clearance Test (in case of *S. saprophyticus*)

with a gram-positive bacteria (*Staphylococcus saprophyticus*, novobiocin resistant) and were sterilized in 70% ethanol. Further, they were cleaned with autoclaved distilled water and lysed in LB (Luria Bertani, lysogeny broth) media using pestles. Furthermore, they were spread on a plate containing LA (Luria Agar, novobiocin resistant). This procedure was repeated after 6 hrs, and colonies were imaged using Syngene G-box.

# Chapter 3 Results and Discussion

One of the main components of this project pertains to verifying the effectiveness of CG17192, an uncharacterized gene. This entails executing procedures such as cloning and expressing in order to observe its biochemical activity. The bulk of my efforts have been dedicated towards designing plasmids and establishing a consistent means for protein expression across various vectors. Additionally, another facet of this undertaking will involve investigating how this particular gene functions within *Drosophila*'s immunity system.

## PCR screening of recombinant plasmids

CG17192, a *Drosophila* gene was extracted from the adult cDNA of *Drosophila melanogaster* (refer to **Figure 6**) using primers mentioned in **Table 3**. and **Table 4** that were designed to have a similar set of bases with the vector. The amplified vector was also digested with Dpn-I and then gel-extracted. Dpn-I is a restriction enzyme that recognizes methylated DNA and cleaves it. In this case, the enzyme would have cleaved any methylated bacterial DNA present in the amplified vector, leaving only the non-methylated vector DNA. Gel extraction refers to the process of isolating DNA fragments of interest from an agarose gel following gel electrophoresis.

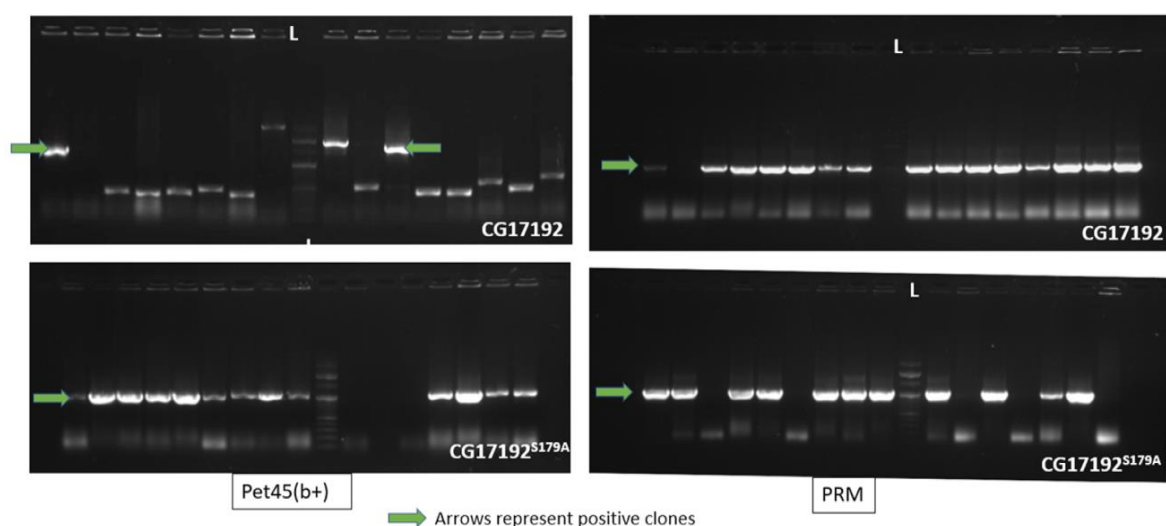


**Figure 11. PCR screening of recombinant Plasmids derived from SLICE** batch cloning of inserts (CG17192, CG17192 S179A) in different vectors like pET45b+ (bacterial expression vector) and pRM (insect expression vector). Forty-four independent colonies (lane 1-80) were subjected to PCR analysis with primer pair (as mentioned in Chapter. 2). Recombinant plasmids pET45b+-6xHis-CG17192, pET45b+-6xHis-CG17192 S179A , pRM-6xHis-CG17192, pRM-6xHis-CG17192 S179A yielded PCR products of ~1kb (lanes labelled with a green arrow).

The gel images (in **Figure 11.**) showed bright bands at a similar length of the amplicon (~1.5 kbp), which suggested that the gene had been inserted into the vector. This is because the expected size of the gene was around 1.5 kbp. However, there were also lower bands below the expected size, which could be due to non-specific binding or the presence of other fragments. The lower bands could also be due to incomplete digestion of the vector with Dpn-I or the presence of residual non-methylated bacterial DNA.

To confirm the successful cloning, the constructs were sent for sequencing. Sequencing is a technique that allows for the determination of the nucleotide sequence of a DNA fragment. By sequencing the cloned gene, it was possible to verify the correct insertion of the gene in the vector and ensure that there were no mutations or errors introduced during the cloning process.

The observation of a point mutation at the 179th position, where a nucleophilic serine residue was mutated to alanine, was made to ensure that the cloned gene was catalytically inactive. This is a common strategy for creating inactive versions of enzymes in order to study their structure and function.

In summary, the observations made in the experiment provided evidence for the successful cloning of the gene CG17192 into expression vectors and mutation of the active site to render the enzyme catalytically dead (inactive). However, the sequencing results were necessary to confirm the correct insertion of the gene in the vector and ensure the accuracy of the cloned sequence.

### **Sequencing confirms the insertion of the inserts in the plasmids**

The sequencing result confirms the correct insertion of the CG17192 & its mutant CG17192<sup>S179A</sup> in the bacterial expression vector (pET45b+) (as shown in **Figure 12**) & insect expression vector (pRM) (see **Figure 13** and **Figure 14**).

The following is a representation of a single PCR product in a chromatogram. Each peak corresponds to a nucleotide in the DNA sequence and has a distinct color code: **A (green)**, **T (red)**, **C (blue)**, and **G (black)**. The initial 20 to 40 bases of the trace are typically indistinct. The sequencing protocols are optimized to provide the most precise peak resolution between 100 and 500 bases in the middle of the trace. In this region, the peaks are sharp and well-separated, and the base calling is the most accurate. As the trace progresses toward the end, the peaks become less distinct and less intense, and the base calling becomes less reliable.

To validate the mutation at the 179th position from Serine to Alanine. A mutation was done using two-step PCR (refer to **Figure 7.**). A mutant was further cloned in a bacterial expression vector, pET45b+, as well as an insect expression vector, pRM. Sanger sequencing has led to the result in a correct insertion of the gene and mutant in the vectors. The sequencing results are shown below:

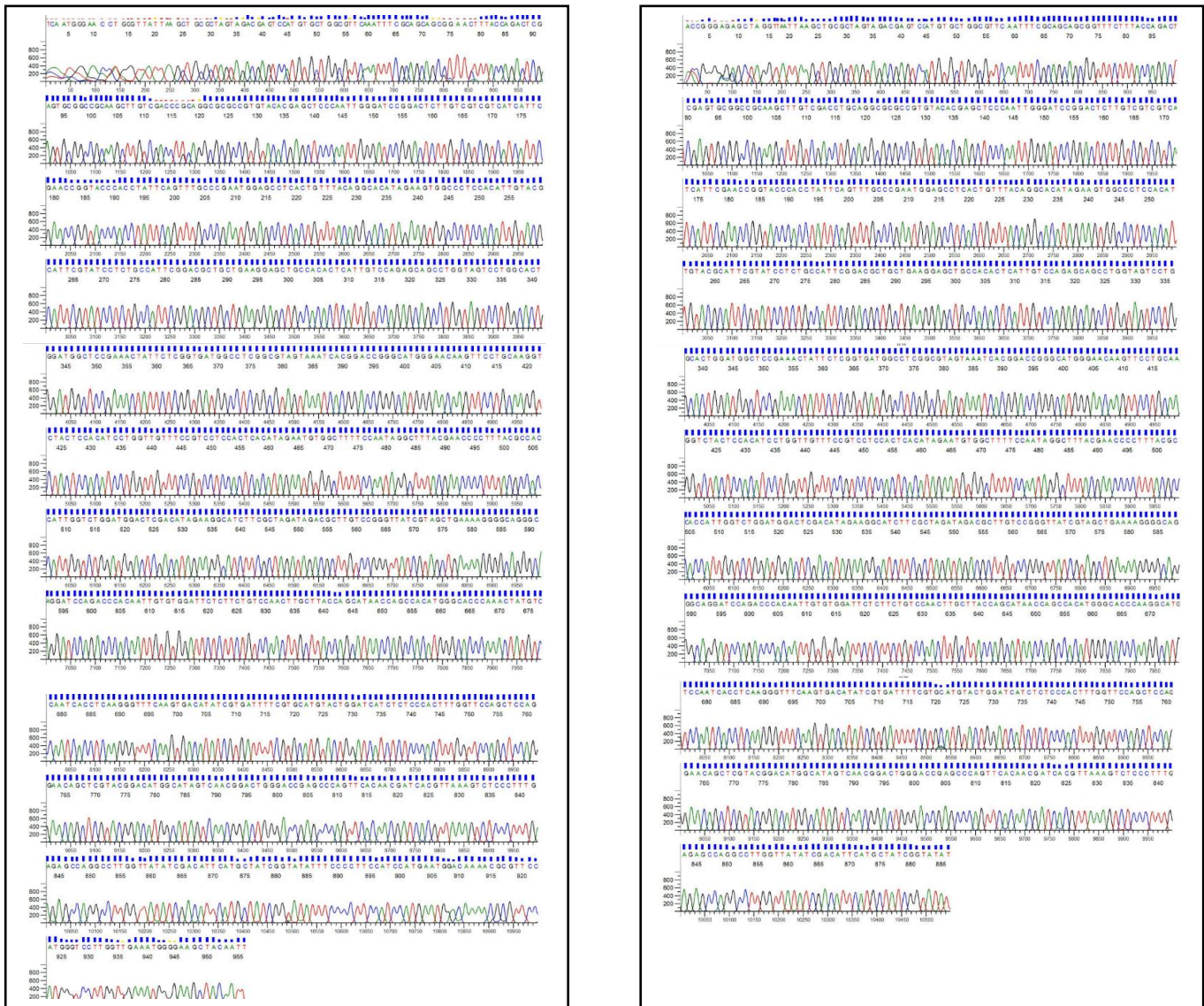


**Figure 12. Sequencing results of the insert in pET45b+** confirm the correct insertion of the gene CG17192 in the vector pet45b+ with a His tag at its N-terminus LEFT. A graph showing the analysis of Sanger sequencing. This sequencing result confirms the correct insertion of CG17192 in the vector pET45b+ which also validates the presence of the 6xHis tag at the N terminus of the CG17192, making the plasmid pET45b+-6xHis-CG17192

Sequencing results confirms the correct insertion of the gene CG17192<sup>S179A</sup> in the vector pet45b+ with a His tag at its N-terminus RIGHT. A graph showing the analysis of Sanger sequencing. This sequencing result confirms the correct insertion of CG17192 in the vector pET45b+ which also validates the presence of the 6xHis tag at the N terminus of the CG17192<sup>S179A</sup>, and also verifies a mutation at the 179th position from serine to alanine, making the plasmid pET45b+-6xHis-CG17192<sup>S179A</sup>

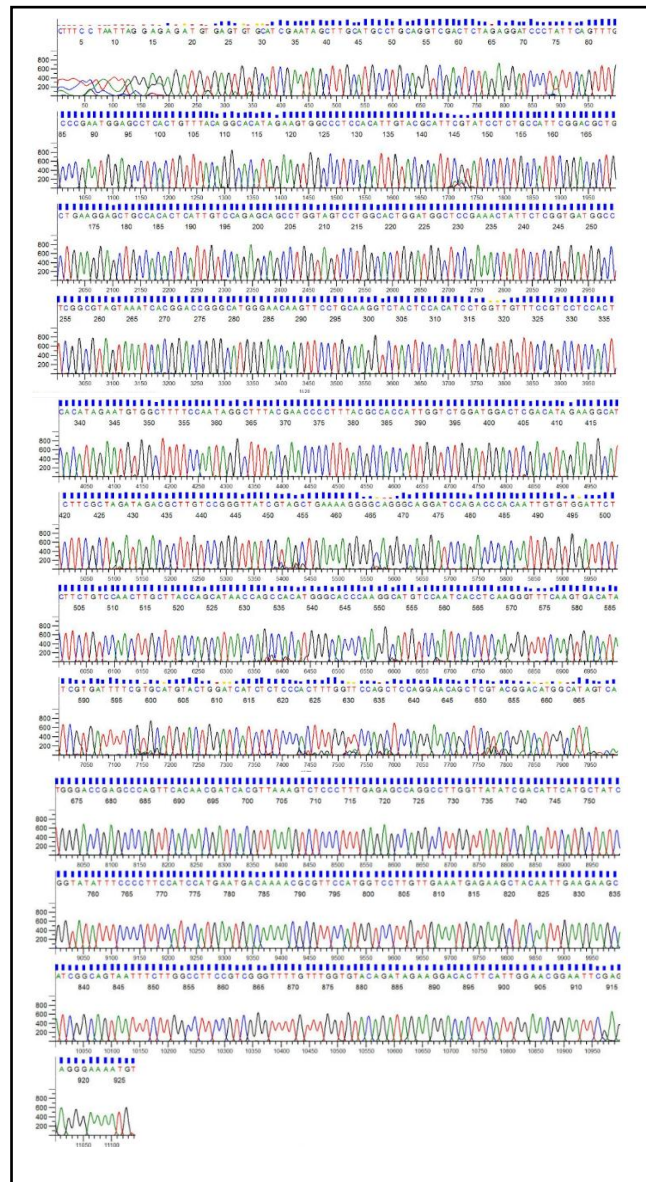
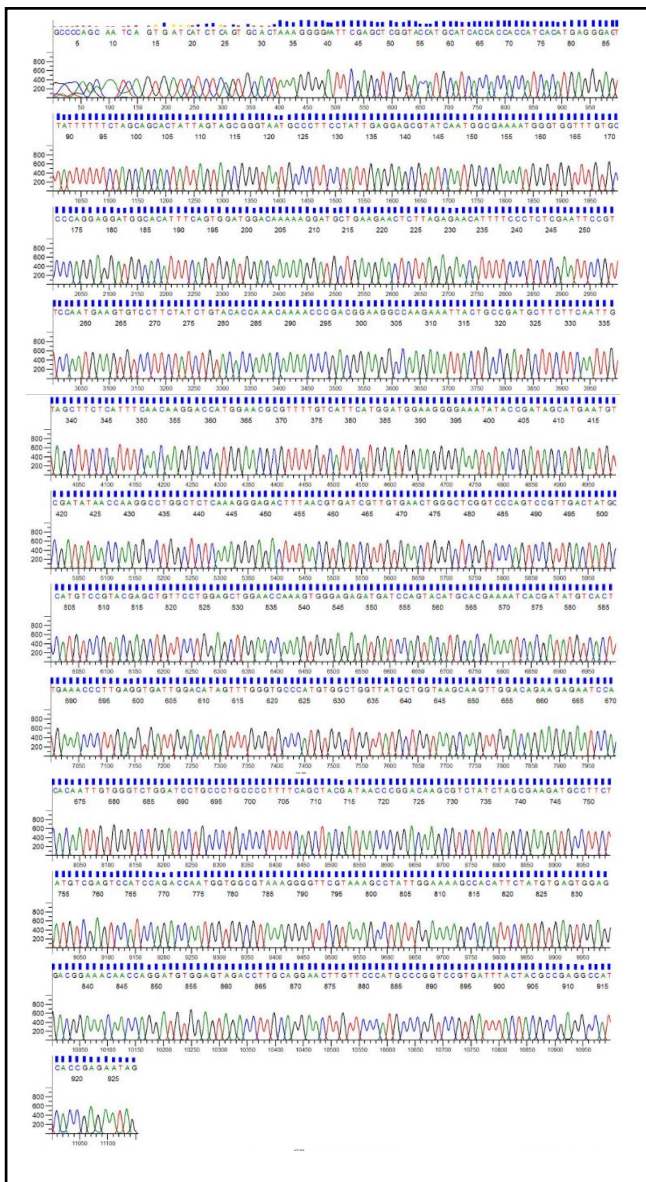


**Figure 13. Sequencing results of the insert in pRM confirms the correct insertion of the gene CG17192 in the vector pRM with a His tag at its N-terminus LEFT.** A graph showing the analysis of Sanger sequencing. This sequencing result confirms the correct insertion of CG17192 in the vector pRM which also validates the presence of the 6xHis tag at the N terminus of the CG17192, making the plasmid pRM-6xHis-CG17192.

Sequencing results confirms the correct insertion of the gene CG17192<sup>S179A</sup> in the vector pRM with a His tag at its N-terminus RIGHT. A graph showing the analysis of Sanger sequencing. This sequencing result confirms the correct insertion of CG17192 in the vector pRM which also validates the presence of the 6xHis tag at the N terminus of the CG17192S179A, and also verifies a mutation at the 179th position from serine to alanine, making the plasmid pRM-6xHis-CG17192<sup>S179A</sup>.

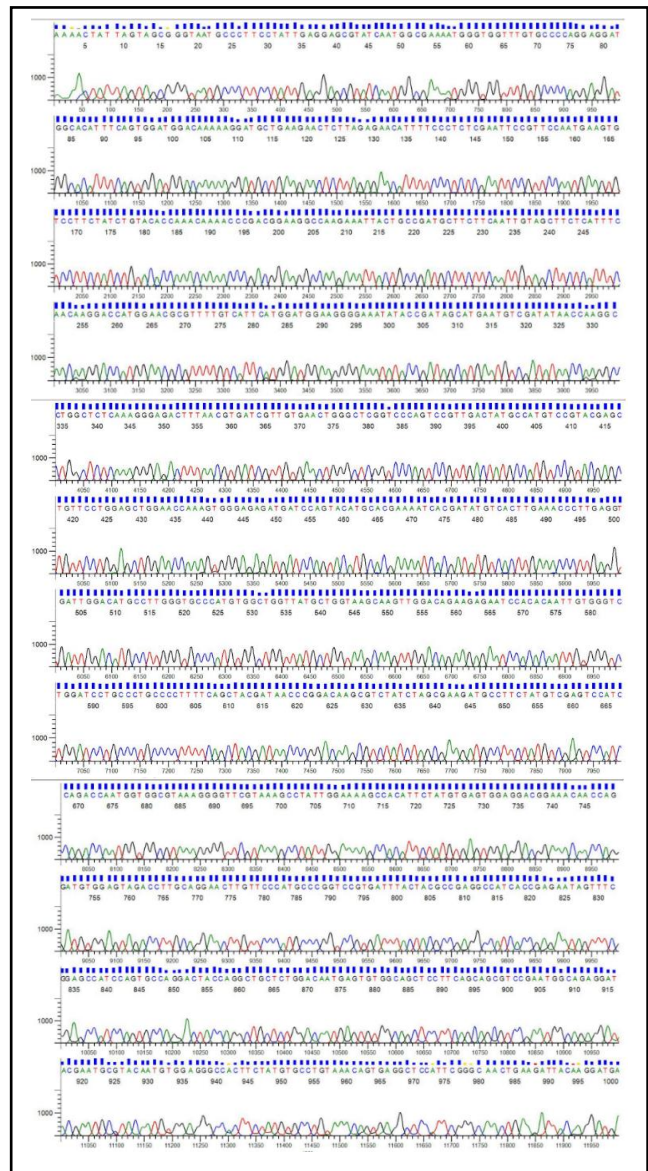
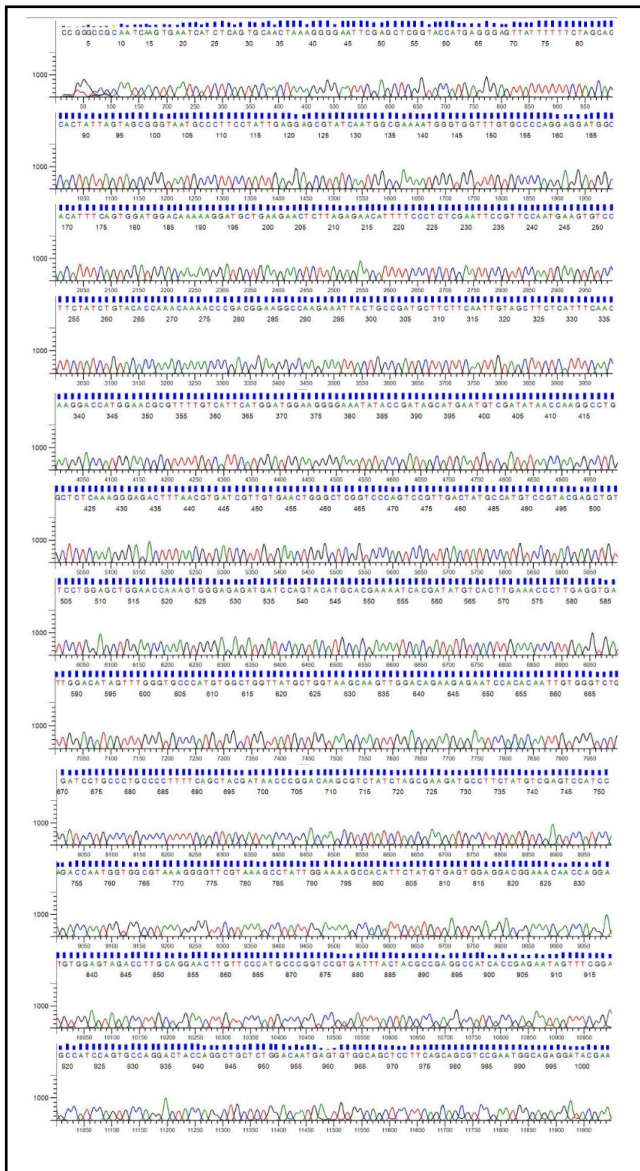


**Figure 14. Sequencing results of the insert in pRM with a FLAG tag confirms the correct insertion of the gene CG17192 in the vector pRM with a FLAG tag at its C- terminus LEFT. A graph showing the analysis of Sanger sequencing. This sequencing result confirms the correct insertion of CG17192 in the vector pRM which also validates the presence of the 1x FLAG tag at the C terminus of the CG17192, making the plasmid pRM-CG17192-1x FLAG.**

Sequencing results confirms the correct insertion of the gene CG17192<sup>S179A</sup> in the vector pRM with a FLAG tag at its C-terminus RIGHT. A graph showing the analysis of Sanger sequencing. This sequencing result confirms the correct insertion of CG17192<sup>S179A</sup> in the vector pRM which also validates the presence of the 1x FLAG tag at the C terminus of the CG17192<sup>S179A</sup> and also verifies a mutation at the 179th position from serine to alanine, making the plasmid pRM-CG17192<sup>S179A</sup>-1x FLAG.

We have successfully cloned the following constructs (refer to **Table 8.**):

1.	pET45b+--6x His—CG17192	2.	pET45b+--6x His—CG17192 <sup>S179A</sup>
3.	pRM--6x His—CG17192	4.	pRM--6x His—CG17192 <sup>S179A</sup>
5.	pRM—CG17192—1x FLAG	6.	pRM—CG17192 <sup>S179A</sup> —1x FLAG

**Table 8. Successfully cloned Constructs**

### Protein expression of CG17192

The plasmids containing CG17192 and CG17192<sup>S179A</sup> were transformed into BL21-De3 cells separately and were induced with IPTG. The cells were grown until the OD<sub>600</sub> reached 0.4-0.6 and then induced with IPTG for 12-16 hours at 18°C. The cells were harvested, and the cellular extracts were obtained by Sonication and centrifugation.

The protein expression of CG17192 and CG17192<sup>S179A</sup> were then analyzed by SDS-PAGE followed by Coomassie staining. The molecular weight of CG17192 and CG17192<sup>S179A</sup> was found to be 37kDa, which is consistent with its predicted molecular weight. However, due to the presence of other proteins in the cellular extracts, it was difficult to distinguish CG17192 and CG17192<sup>S179A</sup> from other proteins based on SDS-PAGE alone.

To address this issue, Western blot analysis was performed using anti-His antibodies. The His-tag was attached to the N-terminus of CG17192 and CG17192<sup>S179A</sup>, allowing for specific detection of the protein. The Western blot analysis confirmed the expression of both CG17192 (as represented in **Figure 15.**) and CG17192<sup>S179A</sup> (as shown in **Figure 16.**) and its molecular weight of 37kDa in the bacterial cells

Overall, the combination of SDS-PAGE, Coomassie staining, and Western blot analysis allowed for the examination of the protein expression of CG17192 and CG17192<sup>S179A</sup> in bacterial cells. The results showed that the protein was expressed and had the expected molecular weight (~37kDa), providing important information for future studies on the function of this protein.



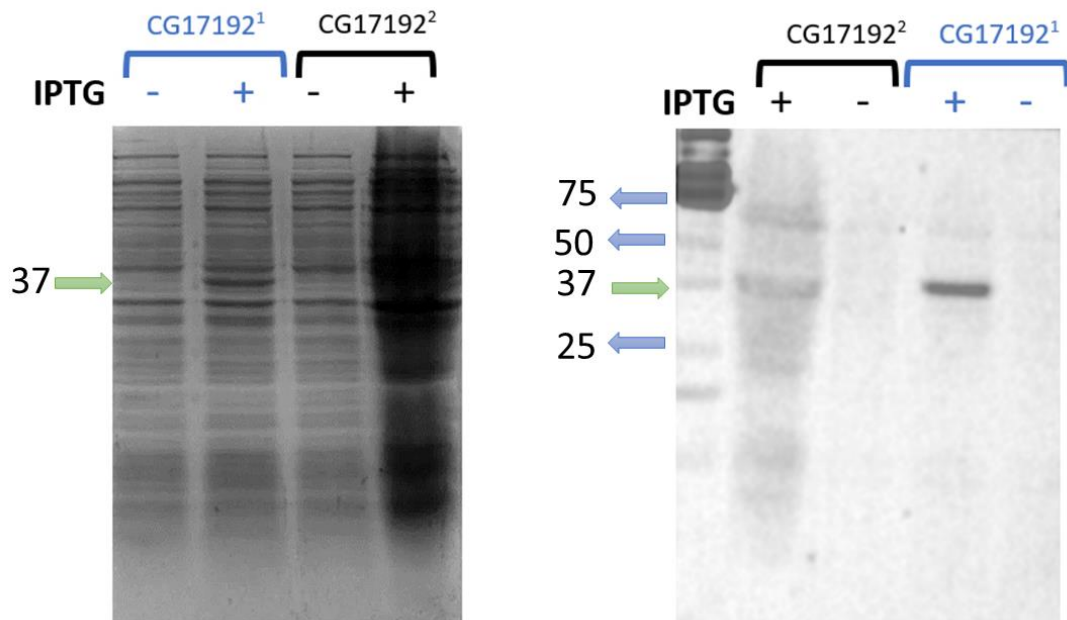


**Figure 15. Western Blot analysis showing protein expression of the wildtype (CG17192) in the bacterial cells, BL21-De3 where 1 & 2 refers to two different wildtype templates. Green arrows in the images depict the protein expression observed at the expected molecular weight (37kDa). IPTG: (Isopropyl  $\beta$ -D-1- thiogalactopyranoside). Primary Antibody: Monoclonal Anti-his tag-mouse (SC-8036) (1:1000); Secondary Antibody: alpha-Mouse HRP (1:10000)**

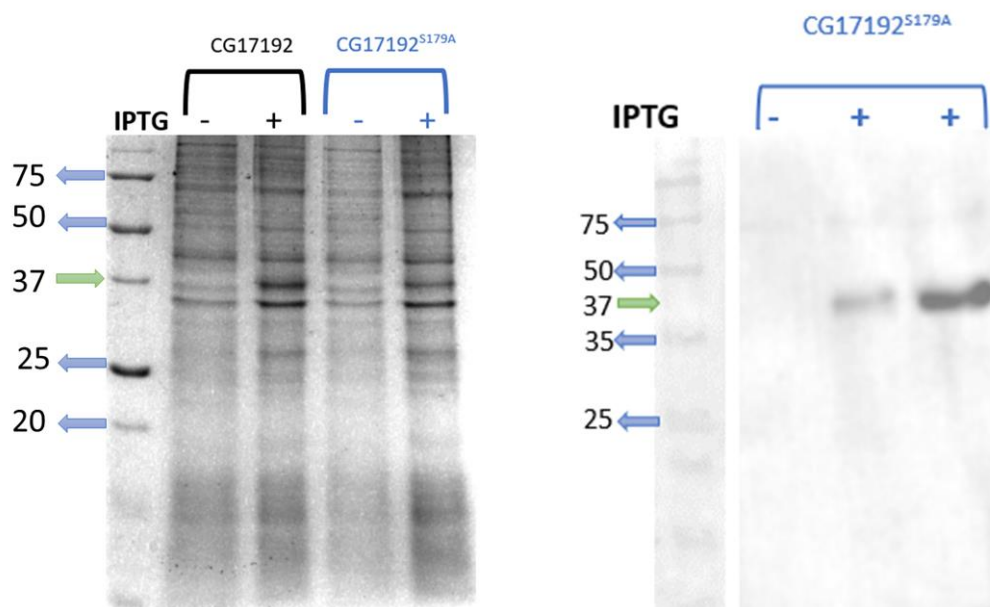


**Figure 16. Western Blot analysis showing protein expression of the mutant (CG17192<sup>S179A</sup>) in the bacterial cells, BL21-De3. Green arrows in the images depict the protein expression observed at the expected molecular weight (37kDa). IPTG: (Isopropyl  $\beta$ -D-1- thiogalactopyranoside). Primary Antibody: Monoclonal Anti-his tag-mouse (SC-8036) (1:1000); Secondary Antibody: alpha-Mouse HRP (1:10000)**

## Detection of CG17192 in the Soluble fraction

The plasmids that had been sequenced were introduced into bacterial cells, specifically BL21-De3, and were allowed to grow at a temperature of 37 °C for approximately 30-40 minutes until the OD<sub>600</sub> reached 0.4-0.6. Following this, the cells were induced with IPTG and kept at a lower temperature of 18 °C for 12-16 hours. The resulting culture was then centrifuged at 6800 rcf for 10 minutes at a temperature of 4 °C. The cellular extracts, or pellets, were then resuspended in 1x PBS and subjected to Sonication for 5 minutes with a pulse of 10 seconds ON and 10 seconds OFF. The cells were further centrifuged at a maximum speed of 10,000 rpm for 40 minutes to separate the supernatant proteome from the pellet proteome, which was then analyzed on 10% SDS PAGE. Subsequently, Western blot analysis

was performed on the soluble proteome (S) and pellet proteome (M) fractions of bacterial cells BL21-De3 using anti-His antibodies to assess the resulting protein expression in the soluble fraction of the extracts.

The results obtained from the SDS-PAGE analysis of the protein fractions obtained after the extraction process are shown in **Figure 17**. A comparison of the SDS-PAGE profiles of the soluble and insoluble fractions showed that some bands with similar molecular weight (MW) were detected in both fractions, while a single band of 37kDa was observed only in the soluble fraction and was not detected in the membrane

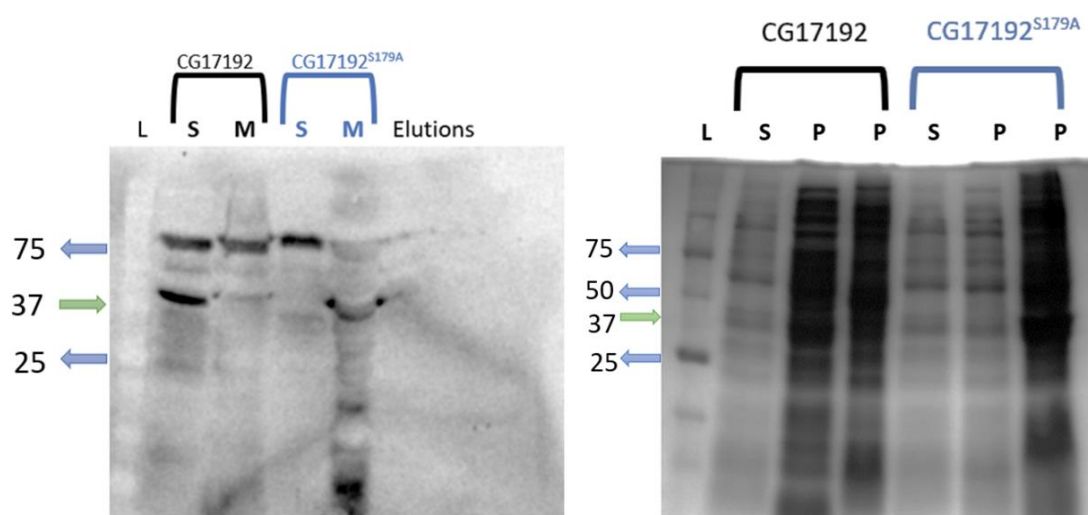


**Figure 17. Immunoblot analysis successfully detects wildtype and mutant in the soluble protein fraction.** Coomassie stained image validates the expression of the protein in the supernatant. A band with an apparent molecular weight of 37kDa was detected in the wild type soluble fraction (Lane-1) but not in the membrane fraction (Lane-2).

IPTG: (Isopropyl  $\beta$ -D-1- thiogalactopyranoside). Primary Antibody: Monoclonal Anti-his tag-mouse (SC-8036) (1:1000); Secondary Antibody: alpha-Mouse HRP (1:10000) b) coomassie stained image which detects wildtype and mutant in the soluble protein fraction. **Green** arrows in the images depict the protein expression observed at the expected molecular weight (37kDa). A band with an apparent molecular mass of 37kDa was detected in the wild type soluble fraction. Here s- soluble fraction; p-pellet fraction; M-membrane fraction; L-ladder.

fraction. The Coomassie-stained gel of protein fractions extracted using different extraction solutions displayed a diverse and complex mixture of proteins with similar banding patterns. However, the western blot increased the sensitivity of the analysis by reducing the mixture of proteins and highlighting only the His-tagged proteins in the mixture. Based on the data obtained from the blot, a band was observed in the supernatant fraction, indicating that the protein was soluble in nature and was present either in the cytoplasm or in the extracellular space. These findings suggest that the extraction method used in this study was effective in separating the protein fractions, and the results obtained from the western blot analysis can be used to identify the specific proteins present in the soluble fraction. Overall, these results provide valuable insights into the nature and location of the proteins present in the extracted fractions, which can be useful in understanding their functional properties and potential applications. However, further studies are required to fully characterize the extracted protein fractions and determine their biological significance.

### Optimizing protein expression of CG17192 in pET45b+

As the purification of CG17192 was not successful due to low expression levels in BL21-De3 cells, We tried to optimize the expression by substituting the bacterial cells with BL21-ai cells. The **Figure 18.** shows that the gene expression was observed in the repressed state when it was transformed into BL21-ai cells, which appeared perplexing. However, upon rechecking the sequence, it was discovered that two start codons were present after the promoter. This finding did not explain the reason for auto-induction but suggested a possible sequence error. The observation that the gene is expressed in the repressed state when transformed into BL21-ai cells is intriguing. The expression of a gene in the repressed state is unexpected, and it raises questions about the underlying reasons for this phenomenon. There could be several reasons why the gene is expressed in the repressed state, including issues with the sequence or environmental factors.

One possibility for the observation is that there are errors in the gene sequence. Two start codons were identified after the promoter, which could have resulted in the expression of the gene in the repressed state. These start codons could have caused

the ribosome to initiate protein translation at an unintended location, leading to the production of truncated proteins or proteins with altered functions.

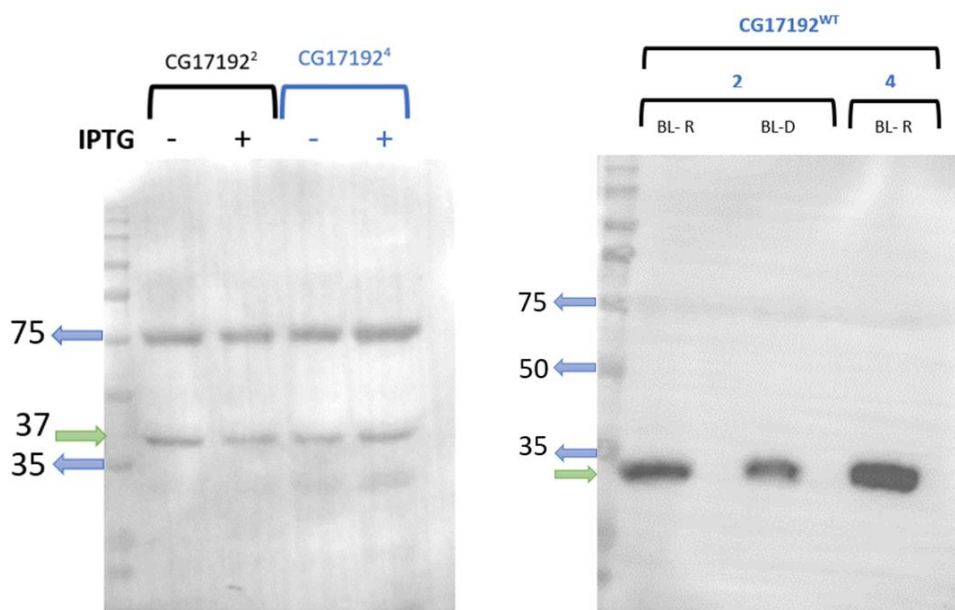


**Figure 18. Western Blot analysis showing protein expression of the CG17192 & mutant (CG17192<sup>S179A</sup>) in the bacterial cells, BL21-ai cells (LEFT) BL21-Rossetta cells (RIGHT). Green arrows in the images depict the protein expression observed at the expected molecular weight (37kDa). While the band in the right figure after pruning a start codon before the His tag is obtained at a lower molecular weight than expected. IPTG: (Isopropyl  $\beta$ -D-1- thiogalactopyranoside). Primary Antibody: Monoclonal Anti-his tag-mouse (SC-8036) (1:1000); Secondary Antibody: alpha-Mouse HRP (1:10000). BL-R represents BL21-Rossetta cells; BL-D represents BL21—De3. 2 and 4 represents similar clones from different colonies.**

This highlights the importance of careful sequencing and optimization of gene constructs before expression studies. Environmental factors can also influence gene expression. The repressed state may contain environmental cues that induce the expression of the gene. Alternatively, the gene may be sensitive to specific environmental factors, such as temperature, pH, or nutrient availability, that are present in the repressed state. To better understand the reason for gene expression in the repressed state, further experiments and analysis are required. For example, the effects of changing the environmental conditions or mutating the gene sequence can be investigated to determine their impact on gene expression. Additionally, a more in-depth analysis of the signaling pathways involved in gene expression in BL21-ai cells may shed light on the mechanisms underlying this phenomenon. In conclusion, the observation of gene expression in the repressed state in BL21-ai cells highlights the complexity of gene expression regulation. Possible explanations for this phenomenon include errors in the gene sequence or environmental factors.

The observation from **Figure 18**. (Right blot), **Figure 19**. and **Figure 20**. highlight the use of pruning to improve protein expression in bacterial cells. The initial construct contained two start codons after the promoter, which resulted in the expression of the gene in the repressed state. However, upon closer inspection, it was found that one of the start codons was after the His-tag, which was causing the issue.

To resolve this, primers were designed to prune the ATG sequence after the His-tag, allowing the protein to be translated with the ATG before the N-terminal His-tag. This strategy resulted in the successful expression of the protein at the expected molecular weight, as observed in the right blot of **Figure 18**.

Further analysis showed that the protein expression was observed at a lower level than the expected molecular weight when the pruned ATG plasmids were used.

However, the wildtype CG17192 enzyme was successfully expressed and purified from E.coli, implying that pruning was an effective strategy for improving protein expression.

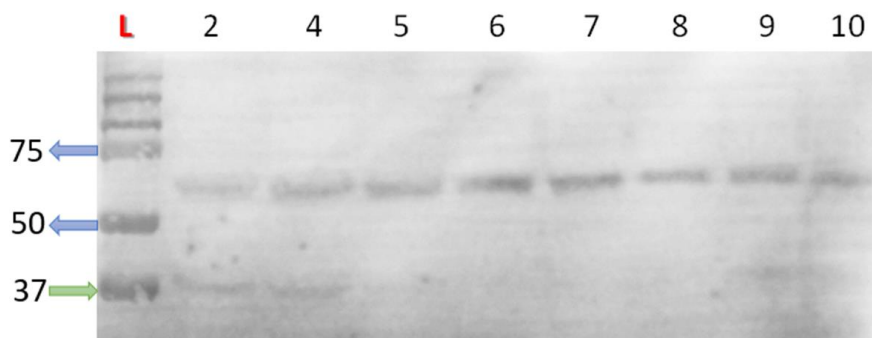


**Figure 19. Western Blot analysis showing protein expression of the CG17192 in the bacterial cells, BL21-Rosetta, after pruning one start codon after the His tag.** Green arrows in the images depict the protein expression observed at the expected molecular weight (37kDa). IPTG: (Isopropyl  $\beta$ -D-1- thiogalactopyranoside). Primary Antibody: Monoclonal Anti-his tag-mouse (SC-8036) (1:1000); Secondary Antibody: alpha-Mouse HRP (1:10000). Here, 2,4,5,6,7,8,9,10 represents similar clones from different colonies.

The application of diverse extraction solutions to obtain protein fractions resulted in the identification of numerous bands exhibiting comparable patterns, as observed through the analysis of Coomassie-stained gel. This observation underscores the intricate nature of characterizing protein mixtures. However, a difference in band pattern was observed at 37kDa, indicating the successful expression of the protein on induction with IPTG.

In conclusion, pruning was an effective strategy for improving protein expression in bacterial cells. The results obtained from this observation demonstrate the importance of careful sequence analysis and optimization in protein expression studies. The use of SDS-PAGE analysis provided a reliable method for assessing protein expression levels and confirming successful protein expression.

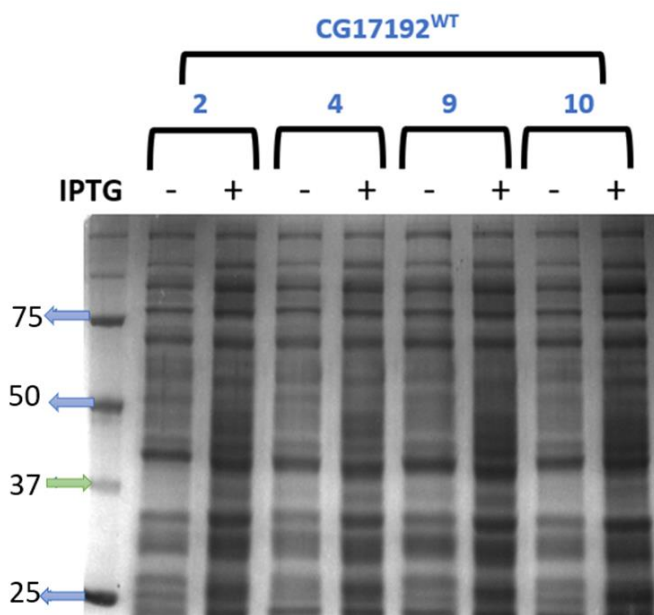


**Figure 20. Coomassie-stained image showing protein expression of CG17192 in the bacterial cells, BL21-Rosetta cells.** Green arrows in the images depict the protein expression observed at the expected molecular weight (37kDa) on induction with IPTG: (Isopropyl  $\beta$ -D-1- thiogalactopyranoside). Here 2, 4, 9, and 10 represent different positive clones of CG17192<sup>WT</sup> after pruning a start codon placed before the His tag at the N terminus of the insert (CG17192). + represent induction, while – represents the repressed state.

### Protein purification of CG17192 using Ni-NTA agarose beads

The process of isolating and purifying proteins is a crucial step in many biological experiments. In this case, the bacterial lysates were resuspended in a Lysis Buffer, followed by Sonication and centrifugation at a maximum speed of 10,000 rpm for 40 minutes. This process was done to separate the pellet proteome from the supernatant proteome. Later, the soluble fraction of the cell lysate was subjected to Ni-NTA agarose beads gel for initial purification of 6x His-CG17192 under native conditions. However, the protein expression was observed not observed in the elutions (in **Figure 21.**) but was obtained in the flowthrough implying that the protein was not binding to Ni-NTA agarose beads. While in elution 3 (of **Figure 22.**) with an imidazole concentration of 500mM, but the band was observed at a lower molecular weight than the expected 37kDa (as shown in **Figure 22.** ). This observation could be due to various reasons,

which are discussed below.

Firstly, the protein may have undergone proteolytic cleavage during the purification process. Proteolytic cleavage is a common phenomenon that occurs during protein isolation and purification, which can cause the protein to break down into smaller fragments. The lower molecular weight band observed could be due to the proteolytic cleavage of the 6x His-CG17192 protein. This cleavage could have occurred during the centrifugation step or the Ni-NTA agarose beads gel purification process.

Secondly, the protein could have undergone denaturation during the purification process. Denaturation is the loss of the protein's native conformation, which can cause changes in the protein's molecular weight. This change in conformation can cause the protein to be more compact or less compact, resulting in a change in the protein's mobility during gel electrophoresis. Denaturation could have occurred during the purification process due to high imidazole concentration, pH changes, or changes in the ionic strength of the solution.

Thirdly, the protein could have been expressed as a truncated protein due to errors in the gene cloning or expression system. The gene cloning and expression system used could have introduced mutations or errors in the 6x His-CG17192 gene sequence, resulting in the expression of a truncated protein. The lower molecular weight band observed could be due to the expression of this truncated protein.

Fourthly, the protein could have undergone post-translational modifications (PTMs) during the purification process. PTMs are chemical modifications that occur after the protein has been translated from the gene sequence. PTMs can cause changes in the protein's molecular weight, conformation, and activity. PTMs can occur due to changes

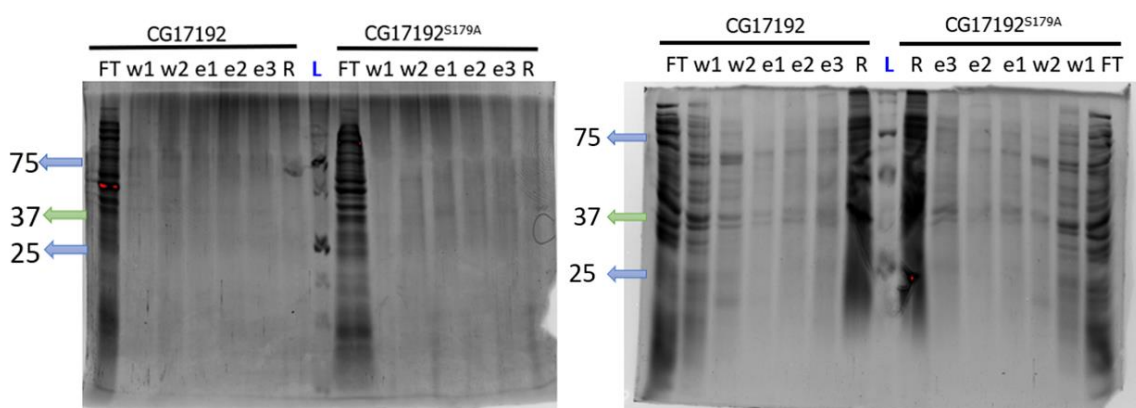


**Figure 21. Purification under Native Conditions.** pET45b+-6x His-CG17192 (wildtype) and pET45b+-6x His-CG17192S179A + (mutant) was expressed in BL21-De3 cells carrying a His tag at its N-terminus and purified using Ni-NTA Agarose beads with different imidazole concentrations in the wash(W1,W2 and W3) and elution (E1,E2 and E3) steps. SDS-PAGE gels were stained by Coomassie Brilliant Blue staining. FT: flow-through; W1: 20 mM Imidazole; W2: 40 mM Imidazole; W3: 60mM Imidazole; E1: 200Mm Imidazole; E2: 400 mM Imidazole; E3: 500mM Imidazole; R: Residual beads. **Green** arrows in the images depict the protein expression observed at the expected molecular weight (37kDa).

in the pH, temperature, or ionic strength of the solution during the purification process. The lower molecular weight band observed could be due to the occurrence of PTMs during the purification process.

In conclusion, the observation of a lower molecular weight band than the expected 37kDa during the purification of 6x His-CG17192 could be due to proteolytic cleavage, denaturation, errors in gene cloning or expression system, or post-translational modifications. Further analysis, such as mass spectrometry, could be used to determine the cause of the lower molecular weight band observed during the purification process. These observations highlight the importance of careful consideration of the protein purification process to obtain pure and intact proteins for downstream applications.

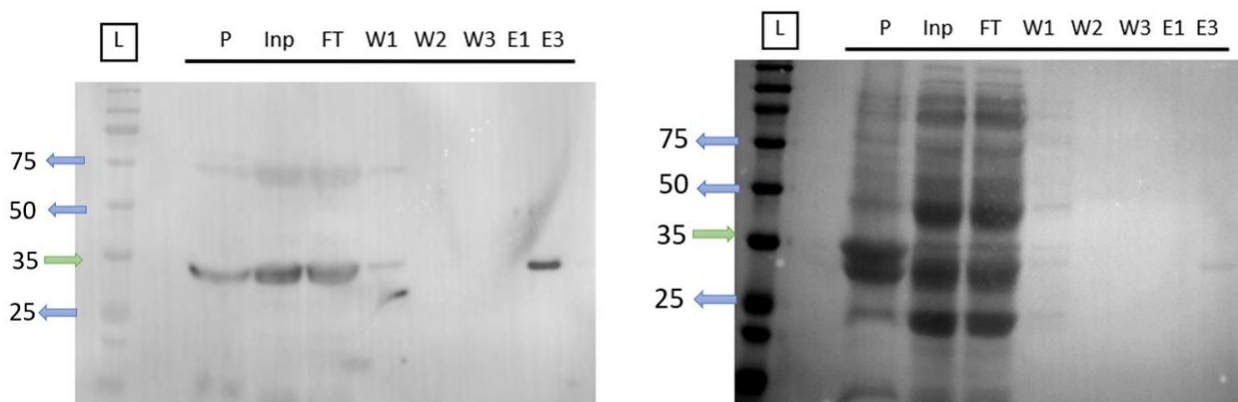


**Figure 22. Immunoblot and ponceau stained blots of protein purification steps.** Lanes: 1) pellet proteome (P) of CG17192 (2) supernatant (Input: Inp) proteome of CG17192 (3) Flow-through (FT) from 2-3 h incubation of pET45b+-6x His-CG17192 protein (lower band) with Ni-NTA resin; (4) Wash 1 (W1) of Ni-NTA resin (with 20mM Imidazole); (5) Wash 2 (W2) of Ni-NTA resin (40mM Imidazole); (6) Wash 3 (W3) of Ni-NTA resin (60mM Imidazole) (7) Elution 1 (E1) of Ni-NTA resin (200mM Imidazole); (8) Elution 3 (E3) of Ni-NTA resin (500mM Imidazole) Primary Antibody: Monoclonal Anti-his tag-mouse (SC-8036) (1:1000); Secondary Antibody: alpha-Mouse HRP (1:10000). **Green** arrows in the images depict the protein expression observed at the expected molecular weight (37kDa).

### **CG17192 is predicted to be secreted in the extracellular space**

The observation in this section pertains to a particular function of this gene (CG17192) which is predicted to be involved in the secretion of lipase enzymes that help in the digestion of triglycerides. The gene contains a signal peptide region (1-16 a.a) and a lipase domain region (16-337 a.a) (as represented in **Figure 23.**). The signal peptide region is responsible for guiding the protein to the secretory pathway, where it is then secreted outside the cell. Once the protein is outside the cell, the signal peptide is cleaved off, and the lipase domain becomes activated to perform its enzymatic



function.

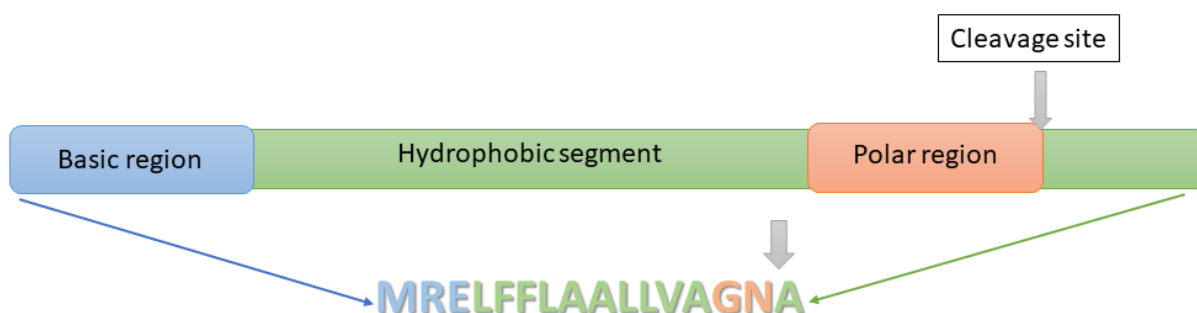


**Figure 23. Signal sequence of CG17192.**

The signal sequence is represented above in which blue color represents the basic region of the amino acid, orange represents the polar region, and green color represents the hydrophobic segment. The alphabets mentioned are the amino acids observed in this sequence. This signal sequence spans 1 to 16 amino acids and is followed by the lipase domain (which spans 36 a.a to 337 a.a)

To confirm the secretory nature of the gene, the constructs were transfected in S2 cells and were incubated for 48 hours. After harvesting the culture at 1000 rcf at 18 °C for 5 min, the media was isolated. Then media was subjected to SDS-PAGE analysis, which separates proteins based on their molecular weight. The SDS-PAGE profiles of the soluble, insoluble, and media fractions were compared, and found that the media fraction and the soluble fraction in both CG17192 and CG17192<sup>S179A</sup> contained a band of higher intensity with a similar molecular weight of 37kDa. These bands were not present in the pellet fraction (see **Figure 24** and **Figure 25**).

The presence of these bands in the media fraction indicates that the protein encoded by the CG17192 gene is secreted out of the cell and present in the media. The absence of these bands in the pellet fraction indicates that the protein is not located within the cells. The four bands with similar molecular weights suggest that the protein is cleaved after the signal peptide region, resulting in a protein fragment with a similar molecular weight.

In conclusion, the observation confirms the secretory nature of the gene CG17192 and suggests that the lipase domain of the protein is activated in the media, where it can perform its enzymatic function. This information can be useful in understanding the

role of the gene in lipid metabolism and potentially developing new therapies for lipid-related disorders.

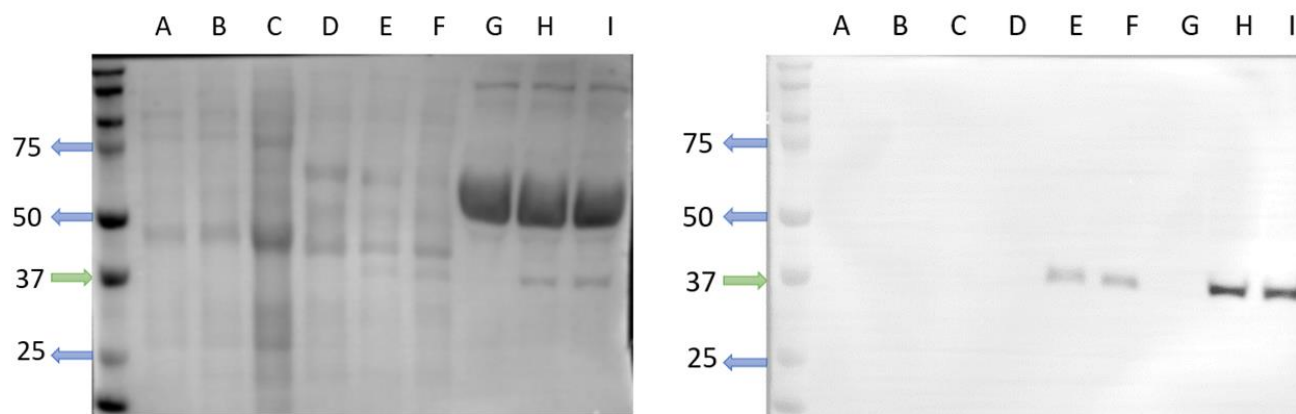


**Figure 24. CG17192 protein expression in transfected S2 cells.** A) Mock does not consist of any plasmids (pellet), B) From S2 cells transformed with pRM-CG17192-1x FLAG (pellet), C) From S2 cells transformed with pRM-CG17192 S179A-1x FLAG (pellet), D) Mock does not consist of any plasmids (supernatant), E) From S2 cells transformed with pRM-CG17192-1x FLAG (supernatant), F) From S2 cells transformed with pRM-CG17192 S179A-1x FLAG (supernatant), G) Mock does not consist of any plasmids (media), H) From S2 cells transformed with pRM-CG17192-1x FLAG (media) I) From S2 cells transformed with pRM-CG17192 S179A-1x FLAG (media). Protein expression was induced by incubating cells in media containing  $\text{CuSO}_4$  for 48 hr at  $25^\circ\text{C}$ . Proteins were separated on a 10% gels, which were stained with ponceau (right) and were used for western blots (left). Western Blots were incubated with a mouse anti-FLAG primary antibody (1:5000 dilution) and an anti-mouse HRP secondary antibody (1:10000 dilution). The molecular weight of the protein standards are shown on the left. **Green** arrows in the images depict the protein expression observed at the expected molecular weight (37kDa).

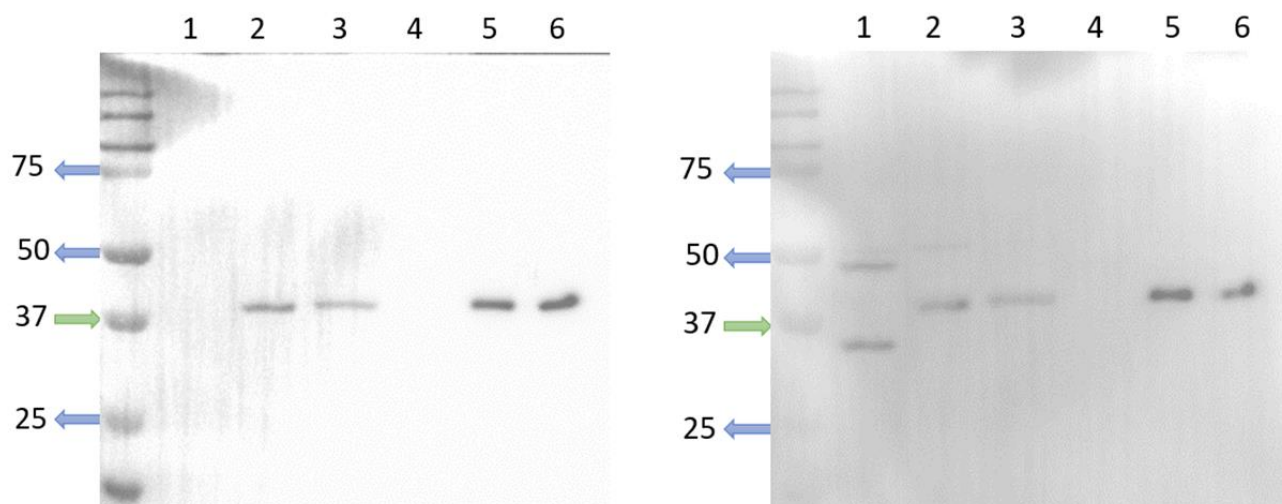


**Figure 25. The SDS-PAGE gel electrophoresis of pRM-CG17192-1x FLAG protein and pRM-CG17192 S179A-1x FLAG.** pRM-CG17192-1x FLAG fusion protein with the size of 37 kDa can be observed. The lanes are samples prepared from soluble fraction of S2 cell lysates: A] using Anti-FLAG Mouse (1) Mock (supernatant), (2) pRM-CG17192-1x FLAG (supernatant), (3) pRM-CG17192 S179A-1x FLAG (supernatant), (4) Mock (media), (5) pRM-CG17192-1x FLAG (media), (6) pRM-CG17192 S179A-1x FLAG (media), B] using Anti-tubulin (1) Mock (supernatant), (2) pRM-CG17192-1x FLAG (supernatant), (3) pRM-CG17192 S179A-1x FLAG (supernatant), (4) Mock (media), (5) pRM-CG17192-1x FLAG (media), (6) pRM-CG17192 S179A-1x FLAG (media). Western Blots were incubated with a mouse anti-FLAG primary antibody with a dilution of 1:5000 and an anti-mouse HRP secondary antibody with a dilution of 1:10000. The molecular weight of the protein standards are shown on the left. The blot (right) was incubated with a mouse  $\alpha$ -tubulin with a dilution of 1:5000 and an anti-mouse HRP secondary antibody with a dilution of 1:10,000. **Green** arrows in the images depict the protein expression observed at the expected molecular weight (37kDa).

## Validation of CG17192 Serine Hydrolase Activity

In order to ascertain the catalytic activity of the S179A mutant, we utilized well-established gel-based ABPP assays. Our findings indicated that while WT CG17192 exhibited substantial activity against the FP-Rhodamine (FP-Rh) probe, no such response was observed for S179A CG17192. These results imply that although the active site-targeted mutation of CG17192 at residue 179 severely impaired its catalytic capacity, it may not have rendered it entirely non-catalytic. To ensure precise protein loading during post-enzyme visualization in gel-based ABPP experiments, Coomassie Brilliant Blue R-250 staining and identical imaging systems were employed. SDS-PAGE analysis of soluble and pellet proteomes from various clones (CG17192 & CG17192 S179A) labeled with SH-directed FP-Rh probes further corroborated our earlier observations regarding the inactivity of the catalytically-compromised S179A variant of this

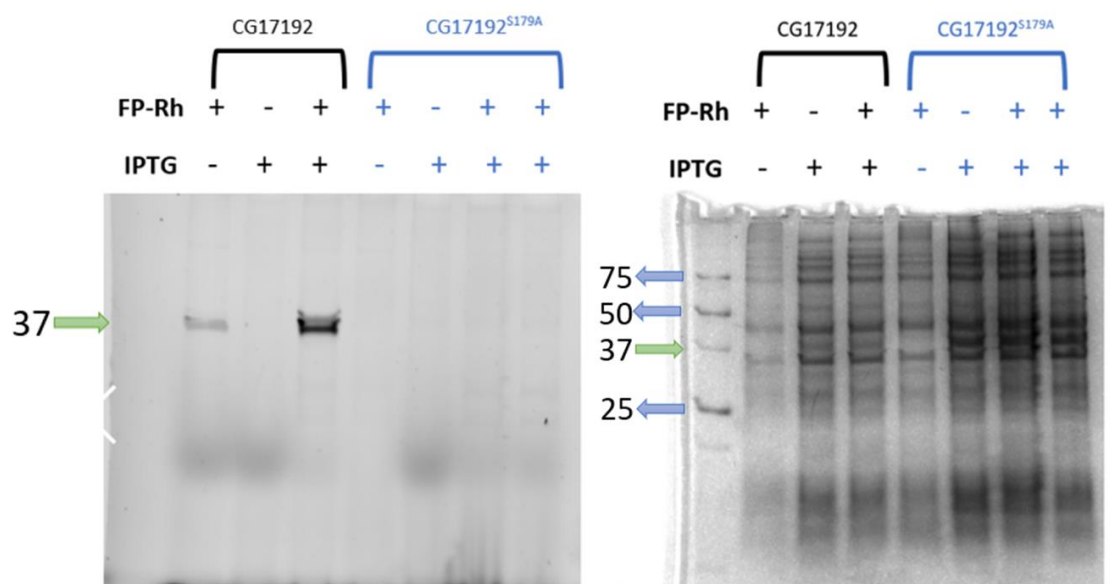


**Figure 26. ABPP Gel image of CG17192 & CG17192 S179A in the bacterial expression vector.** Coomassie Brilliant Blue stained gel image to ensure accurate protein loading. FP-Rh : Fluorophosphonate Rhodamine. (+) & (-) denotes presence or absence of the mentioned reagent respectively. For all the gel-based ABPP experiments, the CG17192 enzyme (either in its wild-type or S179A mutated form) was subjected to treatment with an activity probe consisting of fluorophosphonate-rhodamine (FP-Rh). The resultant enzymatic activity was then observed and recorded utilizing the Syngene Chemi-XRQ gel documentation system. **Green** arrows in the images depict the protein expression observed at the expected molecular weight (37kDa).

enzyme.

To experimentally validate the putative CG17192 catalytic serine residues, we used site-directed mutagenesis to alter the Serine residue to Alanine residue using specific primers and check for loss of activity on an ABPP gel. We modified the target protein such that only one serine was altered to alanine. We used this variant and performed the Biochemical assay, ABPP. Since mutating single serine residue at the 179<sup>th</sup> position, leads to a complete loss of hydrolase activity. We expected that a variant of CG17192 (which is CG17192<sup>S179A</sup>) would show a complete loss of serine hydrolase

activity. As anticipated, the (S→A) mutant shows a complete loss of Serine hydrolase activity with a Fluorophosphonate probe (FP-Rhodamine). This result was validated in bacterial (see **Figure 26**.) and insect cells (refer to **Figure 27** and **Figure 28**).

The observation that the S179A mutant of CG17192 is catalytically inactive is significant, and One possible explanation is that the mutation of serine to alanine at position 179 disrupted the active site of the protein, thereby impairing its ability to carry out its enzymatic function. Serine is an important amino acid in catalytic triads, which are common in hydrolases, and the substitution of serine with alanine may have disrupted

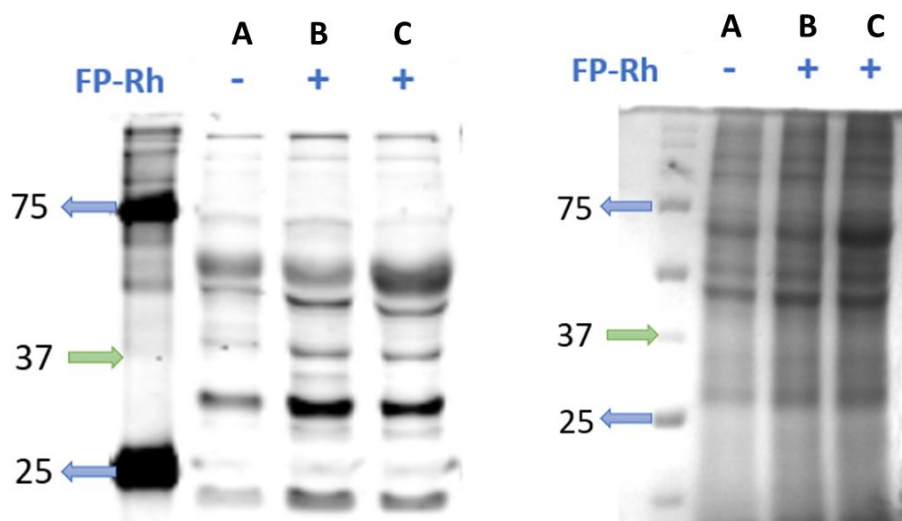


**Figure 27. ABPP Gel image of CG17192 & CG17192<sup>S179A</sup> in the insect expression vector.** Coomassie Brilliant Blue stained gel image to ensure accurate protein loading. FP-Rh : Fluorophosphonate Rhodamine. (+) & (-) denotes presence or absence of the mentioned reagent respectively. For all the gel-based ABPP experiments, the CG17192 enzyme (either in its wild-type or S179A mutated form) was subjected to treatment with an activity probe consisting of fluorophosphonate-rhodamine (FP-Rh). Here, A-mock, B-CG17192 (wildtype), C-CG17192<sup>S179A</sup>. The resultant enzymatic activity was then observed and recorded utilizing the Syngene Chemi-XRQ gel documentation system. **Green** arrows in the images depict the protein expression observed at the expected molecular weight (37kDa).

the proper orientation of the catalytic triad, thereby rendering the enzyme inactive.

It is also possible that the loss of activity in the S179A mutant is due to changes in the protein's conformation or dynamics. Serine hydrolases are known to be highly dynamic and flexible proteins, and it is possible that the substitution of serine with alanine may have altered the protein's flexibility or dynamics, thereby rendering it inactive. Changes in protein dynamics can affect the ability of the protein to carry out its enzymatic function by altering its active site or substrate-binding properties.

The observation that the S179A mutant of CG17192 is catalytically inactive has important inferences for our understanding of the structure and function of serine hydrolases. It suggests that the serine residue at position 179 is critical for the catalytic activity of the protein and that even subtle changes in this residue can have significant

effects on the protein's activity. This finding has important implications for our understanding of the structure and function of serine hydrolases and underscores the importance of site-directed mutagenesis as a tool for studying protein structure and function.

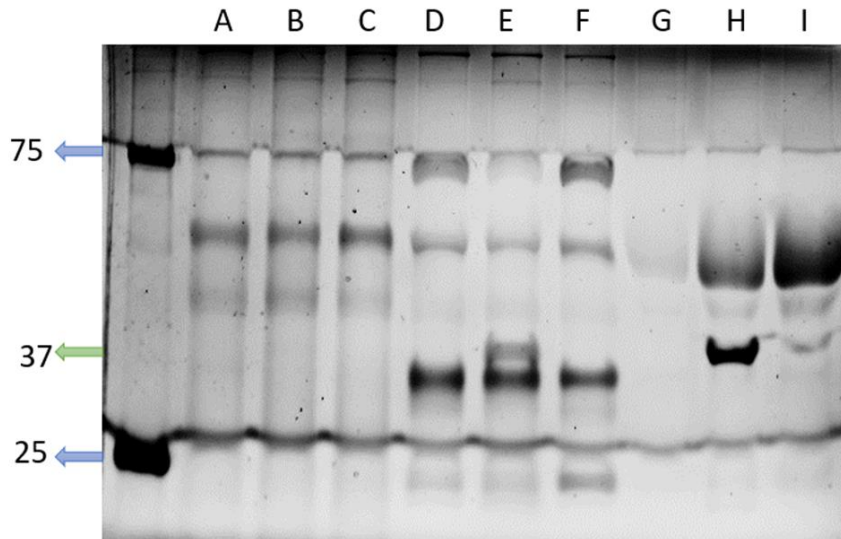


**Figure 28. ABPP Gel image of CG17192 & CG17192<sup>S179A</sup> in the insect expression vector.** A) Mock does not consist of any plasmids (pellet), B) From S2 cells transformed with pRM-CG17192-1x FLAG (pellet), C) From S2 cells transformed with pRM-CG17192<sup>S179A</sup>-1x FLAG (pellet), D) Mock does not consist of any plasmids (supernatant), E) From S2 cells transformed with pRM-CG17192-1x FLAG (supernatant), F) From S2 cells transformed with pRM-CG17192<sup>S179A</sup>-1x FLAG (supernatant), G) Mock does not consist of any plasmids (media), H) From S2 cells transformed with pRM-CG17192-1x FLAG (media) I) From S2 cells transformed with pRM-CG17192<sup>S179A</sup>-1x FLAG (media). Protein expression was induced by incubating cells in media containing CuSO<sub>4</sub> for 48 hr at 25°C. Proteins were separated into 10% gels. The molecular weight of the protein standards is shown on the left. FP-Rh. For all the gel-based ABPP experiments, the CG17912 enzyme (either in its wildtype or S179A mutated form) was subjected to treatment with an activity probe consisting of fluorophosphonate-rhodamine (FP-Rh). The resultant enzymatic activity was then observed and recorded utilizing the Syngene Chemi-XRQ gel documentation system. **Green** arrows in the images depict the protein expression observed at the expected molecular weight (37kDa).

### CG17192 shows immune suppression in the Midgut of the *Drosophila*

The role of CG17192 in regulating gut immunity has not been well-studied. We started by looking at the role of CG17192 in regulating the gut immunity of *Drosophila*. As a first step, we knocked down CG17192, specifically in the Fat Body of the *Drosophila*, using FB-Gal4.

We crossed the FB-Gal4 line to *w<sup>1118</sup>*. In this assay, we introduced a model of systemic infection using a very low dose of *Staphylococcus saprophyticus* (OD<sub>600</sub>: 0.5). We monitored the bacterial load in *w<sup>1118</sup>*, and CG17192<sup>RNAi</sup> flies during gut infection. We crushed each fly separately in sterile PBS and plated appropriate dilutions of the lysate

(to count individual colonies) at 6 hpi.

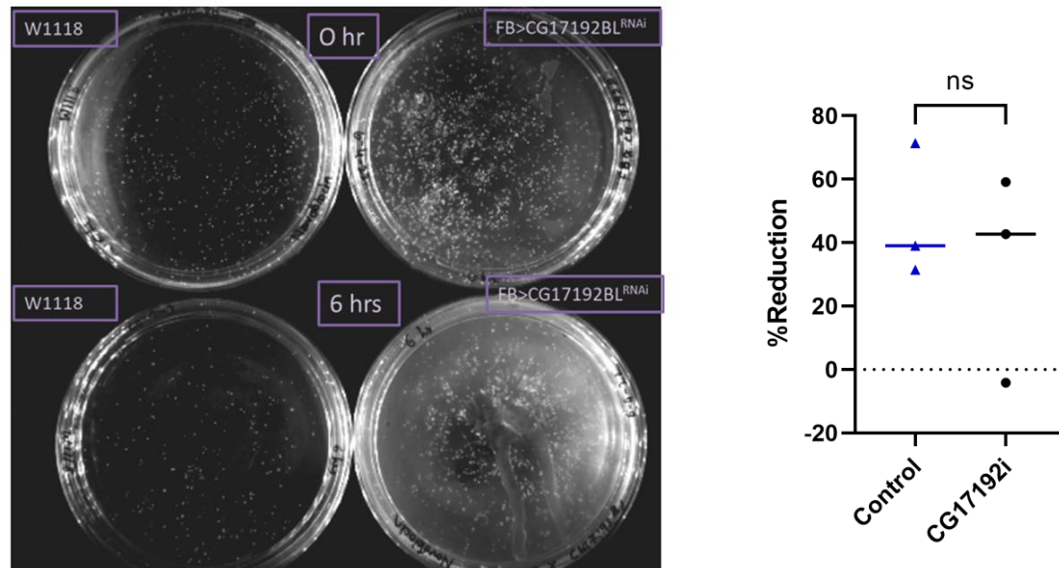


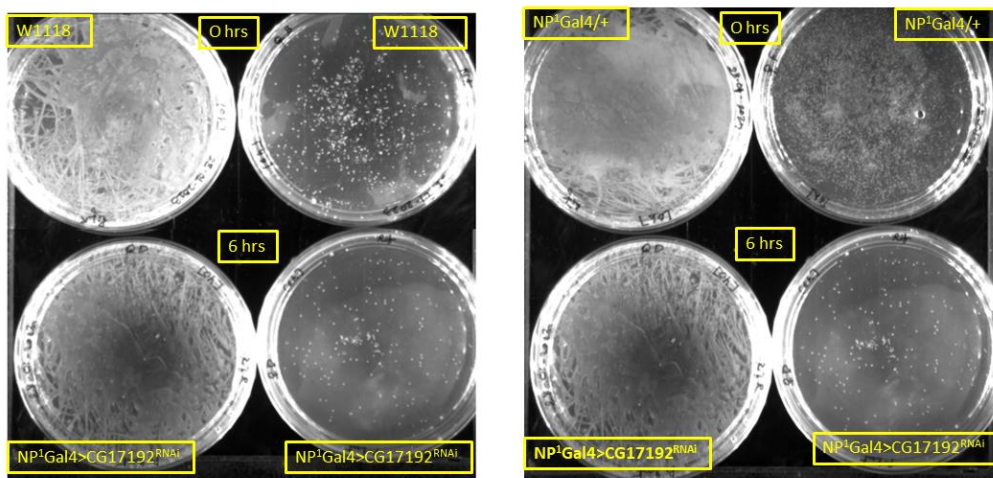
**Figure 29 . Serine Hydrolases Do Not Contribute to the Resistance of *Staphylococcus saprophyticus*.** The plot represents that role of CG17192 is comparable to the wildtype and hence do not contribute much to the Resistance of *Staphylococcus saprophyticus*. Persistence of *S. saprophyticus* in w1118 or CG17192i flies at 0, 6h post-infection. Increased *S. saprophyticus* counts are found in FB>CG17192<sup>BLi</sup> flies after 0 hpi and 6 hpi. The bacterial clearance in case of knockdown flies vs wildtype shows no significant difference. The reduction in the number of colonies for 3 flies 6hpi (hours post infection) is shown on a logarithmic scale while the genotype is on the X-axis. Here, Control-wildtype; CG17192i-RNAi. A statistical analysis using the t-test was conducted to investigate the association between susceptibility to infection by *S. saprophyticus* in wildtype and knockdown flies. The paired t test resulted in a p-value of 0.4485, which strongly supports the assumption that there is no statistically significant difference between the two groups (wildtype versus RNAi)  $t=0.9349$ ,  $df=2$ ,  $P\text{-value}=0.4485$ .

Flies lacking the CG17192 gene (using knockdown RNAi lines) rapidly succumb to infection with a low dose of *S. saprophyticus*. Analysis of the bacterial load of CG17192. We observed that as the time progressed, with infection, CG17192<sup>RNAi</sup> flies were behaving similarly to the wild type. A statistical analysis using the t-test was conducted to investigate the association between susceptibility to infection by *S. saprophyticus* in wildtype and knockdown flies. The paired t test resulted in a p-value of 0.4485, which strongly supports the assumption that there is no statistically significant difference between the two groups (wildtype versus RNAi), thereby indicating normality. The data suggest that the knockdown of CG17192 in the fat body does not lead to any conclusion implying that the role of CG17192 in the Fat Body is not involved in immunity.

The role of CG17192 in regulating gut immunity has not been well-studied. We started by looking at the role of CG17192 in regulating the gut immunity of *Drosophila*. As a first step, we knocked down CG17192, specifically in the enterocytes of the *Drosophila*, using Myo-81F-Gal4<sup>ts</sup> (NP1-Gal4<sup>ts</sup>).

We crossed the NP1-Gal4 line to *w<sup>1118</sup>*. We then orally fed these flies with a gram-negative pathogen, *Pseudomonas entomophila* (P.ent), for 2 hours. We monitored

bacterial load in  $w^{1118}$  and  $CG17192^{RNAi}$  flies during gut infection. The flies were crushed separately in sterile PBS and plated with different dilutions of the lysate (to count individual colonies) at 6 hpi. We observed that as the time progressed, with infection,  $CG17192^{RNAi}$  flies were able to clear bacteria faster than the wild type. This can be noted as increased bacterial clearance as  $CG17192^{RNAi}$  flies have significantly reduced bacterial load at 6 hpi as compared to  $w^{1118}$ . The data suggest that the knock-down of  $CG17192$  in the gut is sufficient to enhance the survival of the flies post-infection. The data results in telling us the possibility that  $CG17192$  might not be involved in the regulation of the toll pathway as it does not respond to gram-positive bacteria (*S.saprophyticus*) but responds to gram-negative bacteria (*P. entomophila*), implying its involvement in the regulation (negatively) of IMD pathway.



### *P. entomophila*

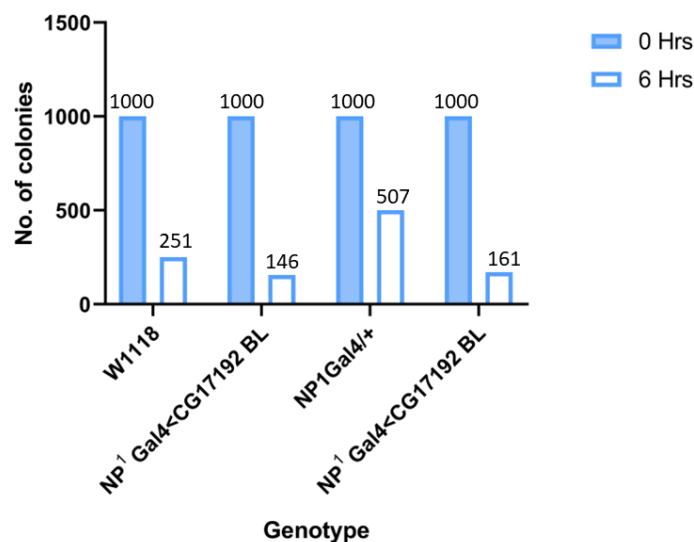


**Figure 30.  $CG17192$  acts as a negative regulator of the host immunity.** The bacterial plates represents that the  $NP1Gal4 > CG17192$  RNAi is clearing bacteria slightly faster than the wildtype and hence contribute to the Resistance of *Pseudomonas entomophila*. We can conclude by saying that  $CG17192$  negatively regulates the immune function of the fly. Persistence of *P.ent* in  $w1118$  or  $CG17192i$  flies at 0, 6h post-infection. Increased *P. ent* counts are found more in  $w1118$  and  $NP1-Gal4/+$  as compared to  $FB>CG17192BLi$  flies after 6 hpi.

The observation that knockdown of CG17192 in the gut enhances the survival of *Drosophila* post-infection with gram-negative bacteria *Pseudomonas entomophila* (*P. entomophila*) (see **Figure 30.**) but not gram-positive bacteria *Staphylococcus saprophyticus* (*S. saprophyticus*) (see **Figure 29**) suggests a possible role of CG17192 in regulating the immune response in the gut.

Firstly, the observation that knocking down CG17192 in the fat body does not affect immunity indicates that its role in immunity is limited to the gut. This implies that CG17192 may be involved in regulating the gut-specific immune response.

Secondly, the finding that knockdown of CG17192 in the gut enhances bacterial clearance in response to *P. entomophila*, but not *S. saprophyticus*, suggests that CG17192 is involved in regulating a specific pathway in the gut immune response. According to the data, CG17192 appears to have a negative regulatory effect on the IMD pathway that combats gram-negative bacteria as part of the innate immune response.

Peptidoglycan recognition proteins (PGRPs) in the intestinal tract activate this particular pathway upon detecting gram-negative bacteria. As a consequence, the activation of NF- $\kappa$ B transcription factors occurs, stimulating the expression of genes crucial for immune response. It is plausible that CG17192 functions as a negative regulator in this pathway by obstructing either NF- $\kappa$ B activation or gene expression involved in this particular cascade.

Lastly, the absence of CG17192 resulted in a faster elimination of bacterial load in *Drosophila* as compared to the wild type. This phenomenon may be attributed to the gene's potential involvement in lipid metabolism or other physiological pathways.

Additional research is required to comprehensively clarify the involvement of CG17192 in controlling the immune response within the gastrointestinal tract. For example, it would be interesting to investigate the expression pattern of CG17192 in the gut and to determine whether it interacts with components of the IMD pathway. Additionally, it would be useful to investigate the effects of overexpression of CG17192 in the gut and its effects on the immune response.

Further studies are needed to fully elucidate the role of CG17192 in regulating the gut immune response and its potential as a target for therapeutic intervention in gut-related infections.



## References

- Bachovchin, DA, Ji, T, Li, W, Simon, GM, Blankman, JL, Adibekian, A, Hoover, H, Niessen, S, and Cravatt, BF (2010). Superfamily-wide portrait of serine hydrolase inhibition achieved by library-versus-library screening. *Proc Natl Acad Sci U S A* 107, 20941–20946.
- Bracey, MH, Hanson, MA, Masuda, KR, Stevens, RC, and Cravatt, BF (2002). Structural adaptations in a membrane enzyme that terminates endocannabinoid signaling. *Science* 298, 1793–1796.
- Braga, PC, Dal Sasso, M, Culici, M, Bianchi, T, Bordoni, L, and Marabini, L (2006). Anti-inflammatory activity of thymol: inhibitory effect on the release of human neutrophil elastase. *Pharmacology* 77, 130–136.
- De Gregorio, E, Spellman, PT, Rubin, GM, and Lemaitre, B (2001). Genome-wide analysis of the *Drosophila* immune response by using oligonucleotide microarrays. *Proc Natl Acad Sci U S A* 98, 12590–12595.
- De Gregorio, E, Spellman, PT, Tzou, P, Rubin, GM, and Lemaitre, B (2002). The Toll and Imd pathways are the major regulators of the immune response in *Drosophila*. *EMBO J* 21, 2568–2579.
- Dinh, TP, Carpenter, D, Leslie, FM, Freund, TF, Katona, I, Sensi, SL, Kathuria, S, and Piomelli, D (2002). Brain monoglyceride lipase participating in endocannabinoid inactivation. *Proc Natl Acad Sci USA* 99, 10819–10824.
- Dodson, G, and Wlodawer, A (1998). Catalytic triads and their relatives. *Trends in Biochemical Sciences* 23, 347–352.
- Gupta, R, Gupta, N, and Rathi, P (2004). Bacterial lipases: an overview of production, purification and biochemical properties. *Appl Microbiol Biotechnol* 64, 763–781.
- Holmquist, M (2000). Alpha/Beta-hydrolase fold enzymes: structures, functions and mechanisms. *Curr Protein Pept Sci* 1, 209–235.
- Kienesberger, PC, Oberer, M, Lass, A, and Zechner, R (2009). Mammalian patatin domain containing proteins: a family with diverse lipolytic activities involved in multiple biological functions. *J Lipid Res* 50 Suppl, S63-68.
- Lane, RM, Potkin, SG, and Enz, A (2006). Targeting acetylcholinesterase and butyrylcholinesterase in dementia. *Int J Neuropsychopharmacol* 9, 101–124.
- Lemaitre, B, and Hoffmann, J (2007). The Host Defense of *Drosophila melanogaster*. *Annual Review of Immunology* 25, 697–743.
- Liu, Y, Patricelli, MP, and Cravatt, BF (1999). Activity-based protein profiling: The serine hydrolases. *Proceedings of the National Academy of Sciences* 96, 14694–14699.
- Long, JZ, and Cravatt, BF (2011). The Metabolic Serine Hydrolases and Their Functions in Mammalian Physiology and Disease. *Chem Rev* 111, 6022–6063.
- Mukherjee, M (2003). Human digestive and metabolic lipases—a brief review. *Journal of Molecular Catalysis B: Enzymatic* 22, 369–376.

Paparazzo, F *Beauveria bassiana* infection in *Drosophila melanogaster*.

Piomelli, D (2003). The molecular logic of endocannabinoid signalling. *Nat Rev Neurosci* 4, 873–884.

Poursharifi, P, Madiraju, SRM, and Prentki, M (2017). Monoacylglycerol signalling and ABHD6 in health and disease. *Diabetes Obes Metab* 19 Suppl 1, 76–89.

Praggastis, SA, Lam, G, Horner, MA, Nam, H-J, and Thummel, CS (2021). The *Drosophila* E78 nuclear receptor regulates dietary triglyceride uptake and systemic lipid levels. *Developmental Dynamics* 250, 640–651.

Ragheb, R et al. (2017). Interplay between trauma and *Pseudomonas entomophila* infection in flies: a central role of the JNK pathway and of CrebA. *Sci Rep* 7, 16222.

Rajendran, A, Vaidya, K, Mendoza, J, Bridwell-Rabb, J, and Kamat, SS (2020). Functional Annotation of ABHD14B, an Orphan Serine Hydrolase Enzyme. *Biochemistry* 59, 183–196.

Savinainen, JR, Saario, SM, and Laitinen, JT (2012). The serine hydrolases MAGL, ABHD6 and ABHD12 as guardians of 2-arachidonoylglycerol signalling through cannabinoid receptors. *Acta Physiologica* 204, 267–276.

Shin, M, Ware, TB, Lee, H-C, and Hsu, K-L (2019). Lipid-metabolizing serine hydrolases in the mammalian central nervous system: endocannabinoids and beyond. *Biochim Biophys Acta Mol Cell Biol Lipids* 1864, 907–921.

Shin, S, Lee, T-H, Ha, N-C, Koo, HM, Kim, S-Y, Lee, H-S, Kim, YS, and Oh, B-H (2002). Structure of malonamidase E2 reveals a novel Ser-cisSer-Lys catalytic triad in a new serine hydrolase fold that is prevalent in nature. *EMBO J* 21, 2509–2516.

Simon, GM, and Cravatt, BF (2010). Activity-based Proteomics of Enzyme Superfamilies: Serine Hydrolases as a Case Study. *J Biol Chem* 285, 11051–11055.

Singh, AK, and Mukhopadhyay, M (2012). Overview of fungal lipase: a review. *Appl Biochem Biotechnol* 166, 486–520.

Soory, A, and Ratnaparkhi, G (2022). SUMOylation of Jun fine-tunes the *Drosophila* gut immune response. *PLOS Pathogens* 18, e1010356.

Valanne, S, Wang, J-H, and Rämetsä, M (2011). The *Drosophila* Toll Signaling Pathway. *The Journal of Immunology* 186, 649–656.

Waring, AL, Hill, J, Allen, BM, Bretz, NM, Le, N, Kr, P, Fuss, D, and Mortimer, NT (2022). Meta-Analysis of Immune Induced Gene Expression Changes in Diverse *Drosophila melanogaster* Innate Immune Responses. *Insects* 13, 490.

Whitcomb, DC, and Lowe, ME (2007). Human pancreatic digestive enzymes. *Dig Dis Sci* 52, 1–17.